بسم الله الرحمن الرحيم

SUDAN UNIVERSITY OF SCIENCE AND TECHNOLOGY

COLLEGE OF GRADUATE STUDIES

Maximum Power Point Tracker of Wind Energy Generation Systems

تتبع نقطة اقصي قدره لنظم التوليد من طاقة الرياح

A Thesis submitted in partial fulfillment for the requirement of the degree of M.Sc. in Electrical Engineering (Power)

Prepared by:

Mohammed Omar Mohammed Ahmed

Supervised by:

Dr. Nagm Aldeen Abdo Mustafa Hassanain

September 2015

الآية

قال تعالي :

((اقْرَأْ بِاسْمِ رَبِّكَ الَّذِي خَلَقَ ﴿١﴾ خَلَقَ الْإِنسَانَ مِنْ عَلَقٍ ﴿٢﴾ اقْرَأْ وَرَبُّكَ الْأَكْرَمُ ﴿٣﴾ الَّذِي عَلَّمَ بِالْقَلَمِ ﴿٤﴾ عَلَّمَ الْإِنسَانَ مَا لَمْ يَعْلَمْ ﴿٥﴾))

صدق الله العظيم

سورة العلق الآيات (من ١-٥)

Dedication

To my parent

To my family

And To my friends

Acknowledgement

First of all Thanks for my God who helped me to complete this project. I would like to express my deepest appreciation to my supervisor **Dr.Nagm Eldeen Abdo Mustafa Hassanian** for all his assistance during this master thesis work, and everybody help me to success of this research

Abstract

Most variable speed wind turbines have pitch angle control mechanisms and one of their objectives is to extract maximum power from available wind speed. By adjusting pitch angles of wind turbine. In this research the use of pitch angle control for wind turbine equipped with self-exited induction generators (SEIGs) and power electronic converters is presented. To extract the maximum available power from the wind, the wind turbine is controlled using pitch angle control based on power signal feedback (PSF) method. The Maximum Power Point Tracking is achieved using two different approaches: The pitch angle control with PI-controller and the pitch angle control with PID-controller. In order to evaluate their performances, both control approaches were tested. The proposed wind generation system has been developed and tested using MATLAB/SIMULINK.

المستخلص

معظم توربينات الرياح تستخدم نظام التحكم في زاوية الخطوه لتوربينة الرياح . حيث ان واحد من اهداف استخدام نظام التحكم في زاوية الخطوه هو الحصول علي اقصي قدرة عند سرعة الرياح المتاحه. بواسطة ضبط زاوية الخطوه . في هذا البحث تم عرض لنظام التحكم في زاوية الخطوه لتوربينة رياح المربوطة الي مولد حثي ذاتي الاثاره وبعض دوائر الكترونيات القدرة ثم الحمل الكهربائي .وللحصول علي اقصي قدره متاحه في سرعة الرياح المعنيه يسخدم نظام التحكم في زاوية الخطوه استناداً علي طريقة التغذية الراجعة لاشاره القدرة .ولانجاز الحصول علي اقصي قدره يستخدم اسلوبين ، نظام التحكم في زاوية الخطوه بالمتحكم التفاضلي التكاملي ونظام التحكم في زاوية الخطوه بالمتحكم التفاضلي التكاملي التناسبي. ومن اجل تقيم واختبار اداء النظام المقترح لتوليد من طاقة الرياح تم اعداد نموزج للنظام واختباره بإستخدم برنامج ماتلاب.

Contents

List of Figures

List of Tables

List of Symbols and Abbreviations

Symbols	Descriptions
V_w	Velocity of wind
C_p	power coefficient
TSR(λ)	Tip speed ratio
$C_{p,opt}$	Optimum power coefficient
λ_{opt}	Optimum Tip speed ratio
P_{max}	maximum mechanical power
Ω	angular rotor speed
R	rotor radius
$v_{cut\text{-}in}$	Cut in of wind speed
$V_{cut\text{-}out}$	Cut out of wind speed
V_r	Rated wind speed
J	moment of inertia
P_m	mechanical power
MPPT	Maximum Power Point Tracking
PSF	power signal feedback
WSM	wind speed measurement
HCS	Hill-Climb Searching
P&O	Perturbation and Observation
ΔP_T	power increment
$\Delta\omega_T$	speed increment
SEIG	Self exited induction generator
B	Pitch angle
P_{ref}	Refines mechanical power
EMI	Electromagnetic Interface
PWM	Pulse width modulation
LC	Inductance capacitance filter

A	swept area
P	Air density
T_m	mechanical torque
T_{haft}	shaft torque
H	Inertia constant
ω_g	angular generator shaft speed
L_m	magnetizing inductance
SSA	state-space averaged
m_i	modulation index
C_D	DC bus capacitor
B_r	Rotor damping effect

CHAPTER ONE

INTRODUCTION

1.1 Introduction

In regulated Due to climate changes such as temperature rise due to increase in greenhouse gases (GHG) emission, increase in sea level, high oil price, depletion of fossil fuel reserves and growing in power demand, the world is obliged to search for new sources of energy on which the emission of (GHG) would be reduced to 5% from their 1990 level. These problems lead scientists towards new clean power conversion systems. The replenished energy resources are suitable to meet the clean power restrictions [1].

Renewable energy resources are promising generation sources for power provider due to advance technology, low production cost, and environmental friendly. Furthermore, cost of fossil fuel is driving force for choosing energy production from renewable energy resources such as wind, solar, biomass etc. Among them wind power has been considered as a strong alternative for traditional power system [2].

Nowadays, the extraction of power from wind at a large scale became a well recognized industry. This fast development of the wind power industry was possible due to several reasons, like: the increasing resistance regarding the use of coal, oil or uranium, the high price of oil and the climate change problem. By the end of 2008, the world total installed capacity of wind turbines reached 122 GW and it is predicted that will exceed 300 GW by the year 2013 [3].

The Major factors that have accelerated the wind-power technology developments are as follows: [4].

• High-strength fiber composites for constructing large low-cost blades.

• Falling prices of the power electronics.

• Variable-speed operation of electrical generators to capture maximum energy.

• Improved plant operation, pushing the availability up to 95 percent.

• Economy of scale, as the turbines and plants are getting larger in size.

• Accumulated field experience (the learning curve effect) improving the capacity factor [4].

The induction machine are presents a well-established technology. The primary advantage of the induction machine is the rugged brushless construction and no need for separate DC field power. The disadvantages of both the DC machine and the synchronous machine are eliminated in the induction machine, resulting in low capital cost, low maintenance, and better transient performance. For these reasons, the induction generator is extensively used in small and large wind farms and small hydroelectric power plants. The machine is available in numerous power ratings up to several megawatts capacity, and even larger [4].

An externally driven induction machine with inappropriate value of capacitor bank can be used as generator. This system is called self-excited induction generator (SEIG). The SEIG has many advantages over the synchronous generator: brushless (squirrel cage rotor), reduced size, rugged and low cost. But the induction generator offers poor voltage regulation and its value depends on the prime mover speed, capacitor bank and load [5].

Distributed power generation has received greater attention in recent years for use in remote and rural communities. Self-excited induction generators have been widely used during the last decades in renewable electric generation especially in wind energy conversion systems (WECS) and hydraulic energy applications in remote isolated areas. Squirrel-cage rotor induction machines are preferred for its reduced cost, robustness, absence of separate source for excitation, and ease of maintenance compared with dc and wound-rotor synchronous machines. Despite these favorable features, induction generators have unsatisfactory voltage and frequency regulation with variation in load (magnitude and power factor) and speed [6].

1.2 Problem statement:

- Problems of wind speed as a variable, this makes electric power generator is variable between high and low depending on wind speed, available where each winds speed available maximum power point, to get to this point is the work of control system of wind energy conversation system, in this project will work a control system is called the maximum point tracking system for wind speed available and will verify the effectiveness of the system to the point of maximum power.

- The change in wind speed makes the voltage generated from energy conversion system is also variable, and this voltage is not suitable for feeding to electrical load, therefore must be make a constant voltage at the electrical load to do so is using control system in power electronic converters.
- Basic problems of wind energy they are not available at all times, and this causes loss of electric generation that supports them, and this lead to the interruption of electrical load, for this reason it is necessary to use emergency power supply units (batteries) with electric power generation from wind energy.

1.3 Objectives:

- The main objective of the thesis is to track and extract maximum power to the loads connected wind energy conversion system using pitch angle control based on power signal feedback (PSF) method by using PI-controller and PID-controller.
- In this project will work to generate electricity from wind energy, where the generating system that has Uninterrupted nutrition (batteries), as well as verify the success of the batteries feeding the electrical load in the event of loss of electric generation from wind energy.
- In this project will work a control system to make the voltage in the electrical load is constant and is not affected by the change of wind speed.

1.4 Methodology:

In this research the mathematical model of wind turbine based on self-excited induction generator is built, and power electronic converters. This complete system is modeled and simulated using Mat lab/ Simulink to extracting maximum power from the wind energy conversation systems (WECS) using power signal feedback (PSF) method by two controllers PI-controller and PID-controller

1.5 Thesis Outline:

This thesis consists of five chapters,

Chapter one: introduction, Problem and objective of research.

Chapter two: presents the Literature review of wind energy, wind turbine, electrical generators, power electronic converter, wind energy conversion system and control of variable speed wind turbine connected to self -exited induction generator (SEIG).

Chapter three: presents the mathematical models of variable speed wind turbine based on self-exertion induction generator.

Chapter four: Applied the pitch angle control based on power signal feedback method to extract maximum power from available wind speed and simulated performance characteristics with the both controllers (PI and PID).

The major Conclusion and the scope of future work are presented in **Chapter five**.

CHAPTER TWO

LITERATURE REVIEW

2.1 Introduction

Wind energy is widely available throughout the world and can contribute to reduced energy import dependence. As it entails no fuel price risk or constraints, it also improves security of supply. Wind power enhances energy diversity and hedges against price volatility of fossil fuels, thus stabilizing costs of electricity generation in the long term [7].

A typical modern wind turbine has one of two basic operating modes: constant or variable speed. The rotor of a constant speed turbine turns at a constant angular speed, often selected so that the generator has the same frequency as the power grid to which it is connected, regardless of wind speed fluctuations. This approach can eliminate the need for expensive power electronics, but it constrains the rotor speed so that the turbine cannot operate at its peak aerodynamic efficiency in all wind speeds. Thus, a constant speed turbine usually produces less power at low wind speeds than does a variable speed turbine, which is designed to operate at a rotor speed proportional to the wind speed (below its rated wind speed) [8].

2.2 Classification of energy resources:

Energy resources can be classified into:

a) Conventional energy resources, which have been traditionally used for many decades, and were in common use around oil crisis of 1973, are called conventional energy resources, e.g. fossil fuels, nuclear, and hydro resources.
b) Non –conventional energy resources, which are considered for large-scale used after the oil crisis of 1973, are called non-conventional energy sources, e.g., solar, wind, biomass, etc [9].

2.3 Importance of non-conventional energy sources:

The concern for environment due to the ever increasing use of fossil fuels and rapid depletion of these resources have led to the development of alternative sources of energy,

which are renewable and environment friendly. Following points may be mentioned in this connection:

1. The demand of energy is increasing by leaps and bounds due to rapid industrialization and population growth, the conventional sources of energy will not be sufficient to meet the growing demand.
2. Conventional sources (except hydro) are non-renewable and bound to finish one day.
3. Conventional sources (fossil fuels, nuclear) also cause pollution thereby their use degrade the environment.
4. Large hydro-resources affect wildlife, cause deforestation and pose various social problems, due to construction of big dams.
5. Fossil fuels are also used as raw materials in the chemical industry (for chemicals, medicines, etc.) [9].

2.4 Worldwide Wind Capacity close to 300 Gig watts in 2013:

The worldwide wind capacity reached 296.255 GW by the end of June 2013, out of which 13980 MW were added in the first six months of 2013. This increase is Signicantly less than in the first half of 2012 and 2011, when 16.5 GW respectively 18.4 GW were added. All wind turbines installed worldwide by mid-2013 can generate around 3.5 % of the world's electricity demand. The global wind capacity grew by 5% within six months (after 7 % in the same period in 2012 and 9 % in 2011) and by 16.6 % on an annual basis (mid-2013 compared with mid-2012). In comparison, the annual growth rate in 2012 was signicantly higher (19 %) [7].

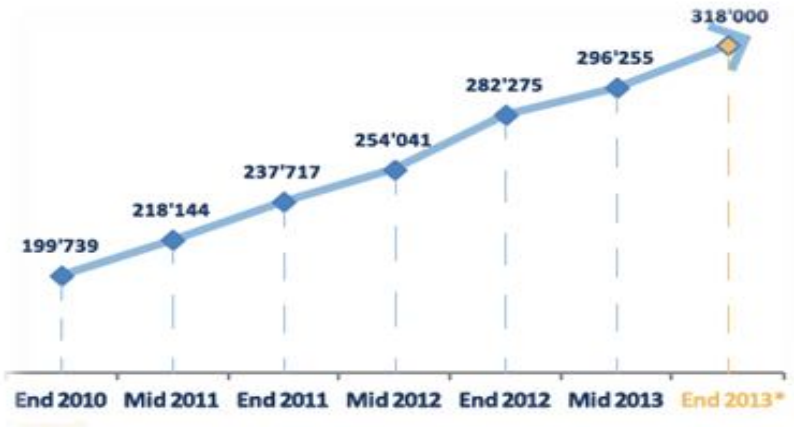

Figure (2.1) Total installed capacity 2010-2013[MW]

2.5 Types of Wind turbines:

Wind turbines can be separated into two types based by the axis in which the turbine rotates. Turbines that rotate around a horizontal axis are more common. Vertical-axis turbines are less frequently used [2].

2.5.1 Horizontal axis wind turbine:

Horizontal-axis wind turbines (HAWT) have the main rotor shaft and electrical generator at the top of a tower, and must be pointed into the wind. Most have a gearbox, which turns the slow rotation of the blades into a quicker rotation that is more suitable to drive an electrical generator [2] [19].

2.5.2 Vertical axis wind turbine (VAWTs):

Vertical-axis wind turbines (or VAWTs) have the main rotor shaft arranged vertically. Key advantages of this arrangement are that the turbine does not need to be pointed into the wind to be effective. This is an advantage on sites where the wind direction is highly variable. VAWTs can utilize winds from varying directions. With a vertical axis, the generator and gearbox can be placed near the ground, so the tower doesn't need to support it, and it is more accessible for maintenance [2] [19].

2.6 Power speed characteristics of wind turbine:

The wind turbine power curves shown in figure (2.2) illustrate how the mechanical power that can be extracted from the wind depends on the rotor speed. For each wind speed there is an optimum turbine speed at which the extracted wind power at the shaft reaches its maximum. The mechanical power transmitted to the shaft is

$$P_w = 0.5\pi\rho R^2 V_w^3 C_p(\beta, \boldsymbol{\lambda}) \qquad (2.1)$$

Where:

$\rho \equiv$ air density .

$R \equiv$ rotor radius of wind turbine .

$V_w \equiv$ wind speed .

$C_p \equiv$ power coefficient .

$\beta \equiv$ pitch angle .

$\lambda \equiv$ ratio of blade tip speed to wind speed (TSR) .

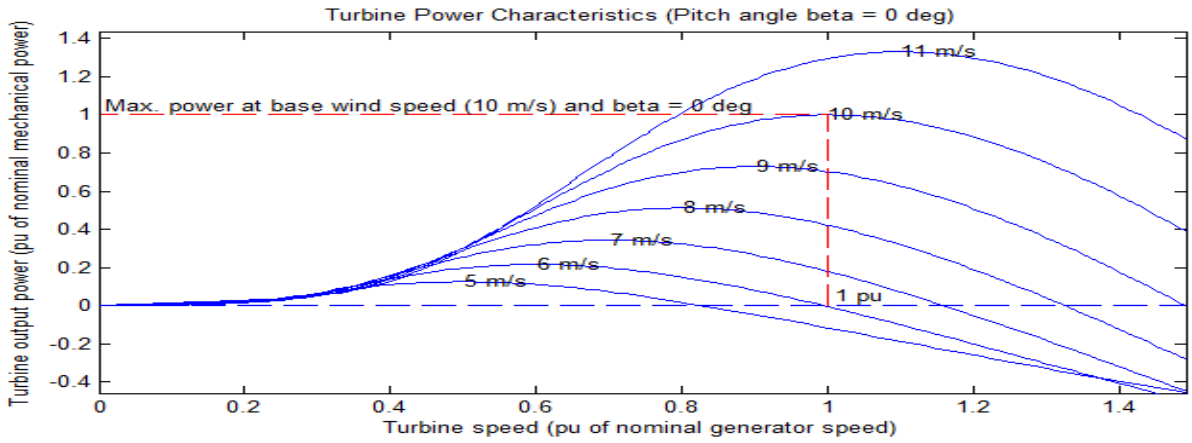

Figure (2.2): Power Speed Characteristics of Wind Turbine

Where is the function of **λ** (T.S.R) and the pitch angle (β)

For a given wind speed, the power extracted from the wind is maximized if C_p is maximized. The optimum value of C_p say $C_{p,opt}$ always occurs at a definite value of λ, say λ_{opt} This means that for varying wind speed, the rotor speed should be adjusted proportionally to adhere always to this value of $\lambda=\lambda_{opt}$ for the maximum power output from the turbine. Using the relation

$$\lambda = \frac{\omega R}{V_w} \qquad (2.2)$$

The maximum value of the shaft mechanical power for any wind speed can be expressed as

$$P_{max} = 0.5\, C_{p,opt}\pi\rho(R^5/\lambda_{opt}^3)\omega^3 \qquad (2.3)$$

Thus the maximum mechanical power that can be extracted from the wind is proportional to the cube of the rotor speed, i.e. P_{max} is proportional to w^3 [2][19]

2.7 Energy captured by wind power conversion system:

A normal wind turbine power curve (power transfer curve) is shown in figure (2.3) with respect to the wind speed. Below the cut in speed ($v_{cut\text{-}in}$), the wind turbine is incapable of meeting fixed losses and so is not operated. As wind speed increases beyond yin, electrical power output rises rapidly. When the wind reaches the speed (V_r), the generator output reaches the rated value. For wind speeds beyond the rated speed, turbine controls act to limit the output power to a constant value either by mechanical control (turbine pitch angle control and/or stall regulation) or by electrical reaction torque

control. Thus the power curve is flat up to wind speed ($\mathbf{V_{cut\text{-}out}}$) where the turbine blades are furled, rotation stops, and the power output drops to zero. It is necessary to furl the machine at very high wind speed to avoid potential irreversible structural damage [3].

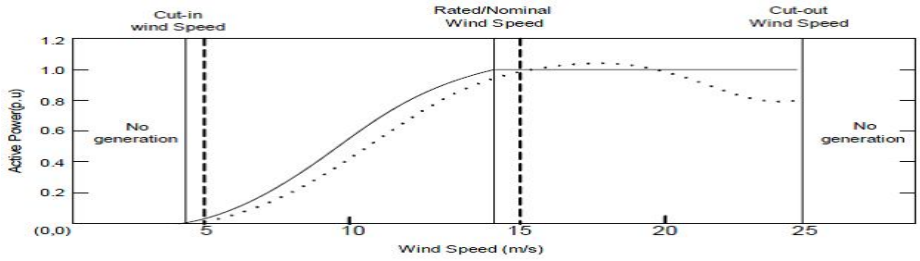

(a)

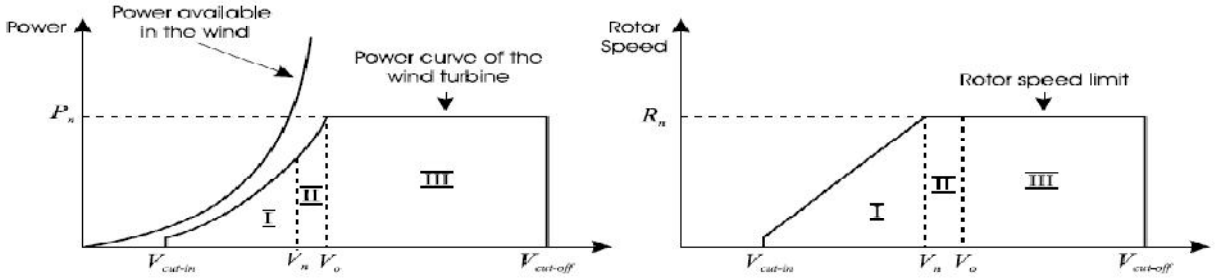

(b)

Figure (2.3): (a) Machine power transfer curve and (b) region of wind turbine

The turbine starts to produce energy when the wind speed is above $V_{cut\text{-}in}$

And stops when the wind speed is below $V_{cut\text{-}off}$

The control of a wind turbine consist three areas:

I. [$V_{cut\text{-}in}$ ... V_n] Area where the turbine operate at "variable-speed" with an optimal rotor speed giving maximal energy.

II. [V_n ... V_o] Operation around rated rotor speed, but below rated power.

III. [V_o ... $V_{cut\text{-}off}$] Turbine operate at full power and rated speed, pitch control active.[10]

2.8 Regions of Control according the wind power curve:

Variable speed wind turbines have three main regions of operation. Figure (2.4) plots the power curves for the wind, an ideal (lossless) turbine, and an example variable speed wind turbine with a 43.3 m rotor diameter. The three major control regions are labeled on the turbine's power curve. In this example, the turbine produces maximum power (800kW) at a rated wind speed of about 14 m/s, and it has a maximum power coefficient $C_{pmax} = 0.4$ [^].

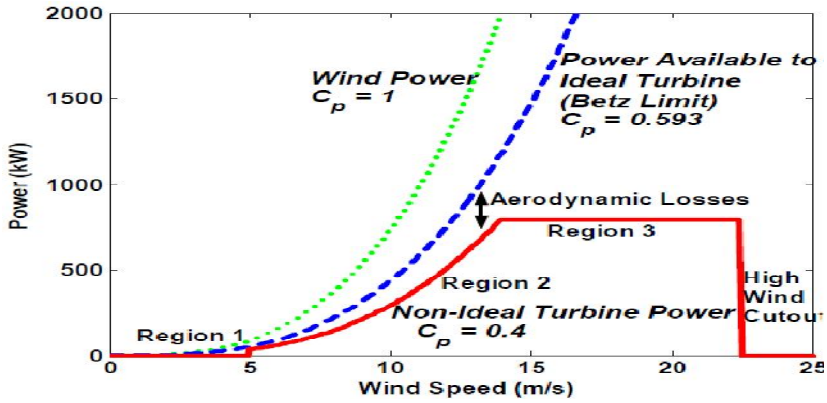

Figure (2.4): Region of machine power transfer curve

Region 1, the section of the solid curve located to the left of 5 m/s wind speed, includes the times when the turbine is not operating and when it is starting up. In general, the region 1 control strategy involves monitoring the wind speed to determine whether it lies within the specifications for turbine operation and, if so, performing the necessary routines used in starting up the turbine. The use of modern control strategies is not usually critical in region 1.

Region 2, shown by the cubic section of the solid curve (approximately 5 to 14 m/s wind speeds), is an operational mode in which it is desirable to capture as much power as possible from the wind. Aerodynamic losses prevent the turbine from achieving its maximum theoretical power extraction from the wind, called the Betz Limit, but the goal is to approach the Betz Limit curve as closely as possible. All three control strategies (yaw drive, generator torque, and blade pitch) may be used in this region; however, it is common to use only generator torque and yaw control for most of the time in region 2, keeping the blade pitch constant at an optimal value for peak energy extraction.

Region 3 operation occurs above rated wind speed, i.e., the wind speed above which maximum peak power is produced. The turbine must limit the fraction of the wind power captured so as not to exceed electrical and mechanical design loads. Thus, the solid curve flattens to the turbine's rated power, 800 kW, above the rated wind speed (approximately 14 m/s). In region 3, a variable speed turbine often maintains a constant speed and constant, rated power, pitching its blades in order to shed additional power. The industry standard control method is proportional- integral-derivative (PID) control on the blade pitch, a simple but effective means for limiting speed and power. Yaw control, generator

torque, and blade pitch strategies can all be used to shed excess power and limit the turbine's energy capture as well as to achieve other control objectives.

2.9 Types of control mechanisms of wind turbine:

Wind turbines have four different types of control mechanisms.

2.9.1 Pitch Angle Control:

In this method there is a mechanism to physically turn the blades around their longitudinal axis. At low wind speed a control system will use this feature to maximize energy extracted from the wind. During the higher wind speed the torque or power can easily be limited to its rated value by adjusting the pitch angle. In addition the axial aerodynamics forces are reduced. This method is almost always used with variable speed turbines in order to make operation at high wind speed possible and safety. On a pitch controlled wind turbine the electronic controller checks the power output of the turbine constantly. When the power output becomes too high, it requested the blade pitch mechanism to immediately turn the blades slightly out of the wind. When the wind speed is less strong the blades are turned back, into the most effective position.[12]

2.9.2 Stall Control:

- ***Passive stall control***:

Generally, stall control to limit the power output at high winds is applied to constant-pitch turbines driving induction generators connected to the network. The rotor speed is fixed by the network, allowing only 1-4% variation. As the wind speed increases, the angle of attack also increases for a blade running at a near constant speed. Beyond a particular angle of attack, the lift force decreases, causing the rotor efficiency to drop. This lift force can be further reduced to restrict the power output at high winds by properly shaping the rotor blade profile to create turbulence on the rotor blade side not facing the wind [12].

- ***Active stall control:***

In this method of control, at high wind speeds, the blade is rotated by a few degrees in the direction opposite to that in a pitch controlled machine. This increases the angle of attack,

which can be controlled to keep the output power at its rated value at all high wind speeds below the furling speed [12].

2.9.3 Power Electronic Control:

In a system incorporating a power electronic interface between the generator and load (or the grid), the electrical power delivered by the generated to the load can be dynamically controlled. The instantaneous difference between mechanical power and electrical power changes the rotor speed following the equation

$$J\frac{d\omega}{dt} = P_m - P_e \qquad (2.4)$$

Where J is the polar moment of inertia of the rotor, ω is the angular speed of the rotor, is the P_m mechanical power produced by the turbine, and P_e is the electrical power delivered to the load [12].

2.9.4 Yaw Control

Turbine is continuously oriented along the direction of the wind flow. This is achieved with a tail-vane in small turbines, using motorized control systems activated either by fan-tail, in case of wind farms, by a centralized instrument for the detection of the wind direction. It is also possible to achieve yaw control without any additional mechanism, simply by mounting the turbine downwind so that the thrust force automatically pushes the turbine in the direction of the wind.

Speed of the rotor can also be controlled using the yaw control mechanism. The rotor is made to face away from the wind direction at high wind speeds, thereby reducing the mechanical power. Yawing often produces loud noise, and it is restriction of the yawing rate in large machines to reduce noise is required [12].

2.10 Maximum Power Point Tracking Control Methods

Three common MPPT methods namely, perturbation and observation (P&O), wind speed measurement (WSM), and power signal feedback (PSF). In the following, these three methods are briefly explained [12].

2.10.1 Perturbation and Observation Method

The Perturbation and Observation (P&O) or Hill-Climb Searching (HCS) method is based on perturbing the turbine shaft speed in small steps and observing the resulting

changes in turbine mechanical power. The concept and schematic diagram of the P&O method is shown in Figure (2.5). If the shaft speed increment ($\Delta\omega_T$) results in a turbine power increment (ΔP_T), the operating region is in the up-hill curve, and increasing shaft speed must be continued toward maximum power point; otherwise, the turbine operating region is in the down-hill curve, so the shaft speed should be decreased by the P&O method to reach the maximum power point. To implement the P&O method, one can check the signs of ($\Delta\omega_T$) and ($\Delta P_T/\Delta\omega_T$). The shaft speed is incremented ($\Delta\omega_T>0$) in small steps as long as ($\Delta P_T/\Delta\omega_T>0$ or decremented ($\Delta\omega_T<0$) in small steps as long as ($\Delta P_T/\Delta\omega_T<0$. This is continued till maximum power point is reached, i.e., ($\Delta P_T/\Delta\omega_T=0$. If incrementing shaft speed results in ($\Delta P_T/\Delta\omega_T<0$ or decrementing shaft speed results in ($\Delta P_T/\Delta\omega_T>0$, the direction of shaft speed change must be reversed

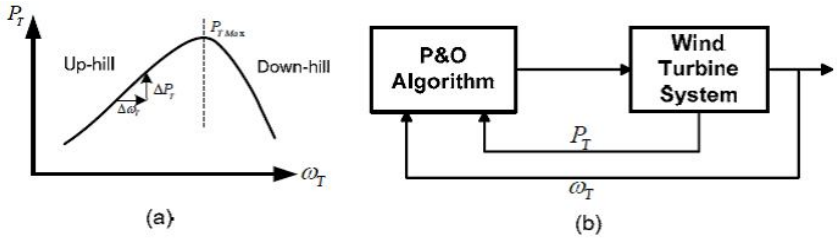

Figure (2.5): P&O method: (a) turbine power versus shaft speed and principle of the P&O method (b) block diagram of the P&O control in wind turbine

2.10.2 Wind Speed Measurement Method

The aim of the turbine speed control is to maintain turbine shaft speed at optimal value, i.e., ω_{max} , P_{max} so that maximum mechanical power can be captured at any given wind velocity (V) In the wind speed measurement (WSM) method, both wind velocity and shaft speed (ω_T) should be measured. Also, optimal tip-speed ratio (λ_{opt}) must be determined for the controller. The block diagram of this method is shown in Figure (2.6).

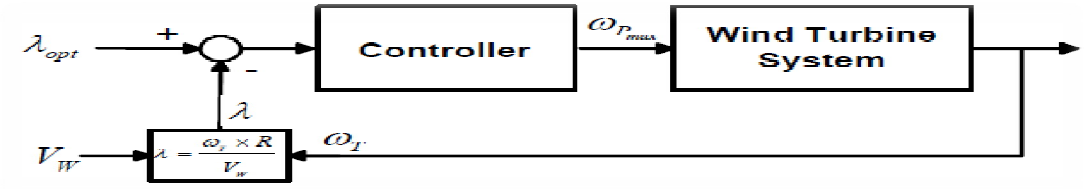

Figure (2.6): Block diagram of a wind energy system with shaft speed control using wind WSM method

Although this method is a simple method for implementing the MPPT, there are two drawbacks to implementing the WSM method. First, obtaining accurate value of the wind velocity is complicated and increases the cost of the system. Second, the optimal tip-speed-ratio is dependent on the wind energy system characteristics. Therefore, the controller will require adjustment before installation in a new wind energy system.

2.10.3 Power Signal Feedback (PSF) Control

The block diagram of a wind energy system with PSF control is shown in Figure (2.7). In this method, the maximum power curve of the wind turbine, Figure (2.7), should be obtained first from experimental results. Then, the data points for maximum output power and the corresponding wind turbine speed must be recorded in a lookup table.

The concept of the PSF method is illustrated in Figure (2.8). Tracking of the maximum power curve, the dashed-curve, is the aim of the PSF method. Suppose the system is initially stable at point A with wind velocity V_1, shaft speed ω_{T1} and maximum output power P_1. If the wind velocity increases to V_0, the new optimum power targeted by the controller should be P_0. In the moment following the wind velocity change, the shaft speed is still at ω_{T1}, due to inertia of the shaft. But, the turbine output power is increased to P'_1, while the power reference based on the lockup table is still P_1. The shaft will accelerate under additional turbine torque and the operating point is moved by the controller on the P_T-ω_T curve corresponding to V_0 toward point B. eventually, the system will stabilize at point B with the new output power P_0. Similar to this scenario, if the system is settled down initially at point C and the wind velocity decrease to the V_0, the shaft decelerates toward ω_{T0}.

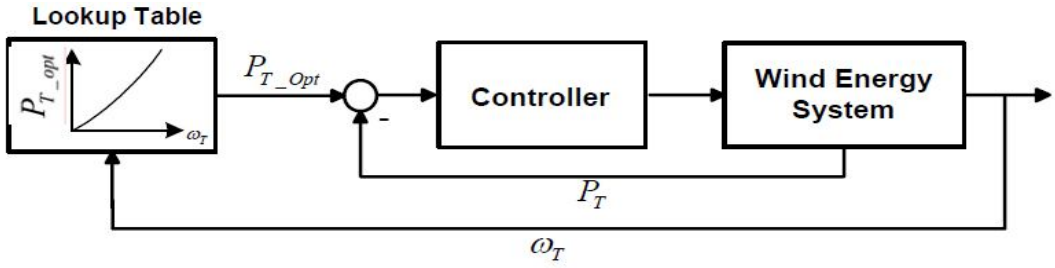

Figure (2.7): Block diagram of a wind energy system with Power Signal Feedback control

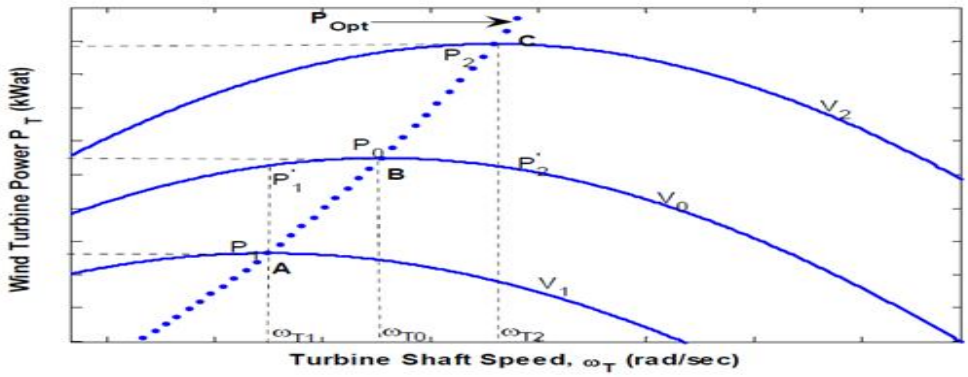

Figure (2.8): wind turbine power versus turbine speed

2.11 Electrical Generator used in wind generation system

The conversion of the mechanical power of the wind turbine into the electrical power can be accomplished by any one of the following types of the electrical machines:

- The direct current (DC) machine.
- The synchronous machine.
- The induction machine [4].

2.11.1 Induction Machine

Traditionally, synchronous generators have been used for power generation but induction generators are increasingly being used these days because of their relative advantageous features over conventional synchronous generators. These features are brush less and rugged construction, low cost, maintenance and operational simplicity, self-protection against faults, good dynamic response, and capability to generate power at varying speed. For its simplicity, robustness, and lower cost, the induction generator is favored for small hydro and wind power plants. The need of external reactive power to produce a rotating flux wave limits the application of an induction generator as a stand-alone generator. However, it is possible for an induction machine to operate as a self-excited induction generator (SEIG) if capacitors are connected to the stator terminals to supply sufficient reactive power.

2.11.1.1 Classification of induction generators

The induction machine offers advantages for hydro and wind power plants because of its easy operation as either a motor or generator, it has different application in different

areas, and depending upon them it has many classifications. Induction generators can be classified on the basis of excitement process as

- Grid connected induction generator
- Self-excited induction generator

Further induction generators are classified on the basis of rotor construction as

- Wound rotor induction generator
- Squirrel cage induction generator

Depending upon the prime movers used and their locations, generating schemes can be broadly classified as under [4].

- Constant speed constant frequency [CSCF]
- Variable speed constant frequency [VSCF]
- Variable speed variable frequency [VSVF]

2.11.1.2 Induction generator principle

An induction machine rotating with the speed higher than that of the magnetic field of the stator operates as a generator, feeding electrical power back to the supply system. When the speed of the rotor is above the speed of the magnetic field (synchronous speed), the slip goes to a negative value which makes the developed torque to become negative. Thus the machine absorbs real power from the shaft and develops electric power yielding to generator operation. This property is utilized in, for example, induction generators driven by a wind turbine and connected to the grid [13].

2.11.1.3 Phenomena of self-excitation

When the induction machine is driven by a prime mover, the residual magnetism in the iron core of the magnetic circuit of the machine induces EMF in the stator windings at a frequency proportional to the rotor speed. This EMF is applied to the capacitors connected to the stator terminals and causes leading current to flow in the stator winding, and hence a magnetizing flux in the machine is established. Thus the self-excitation process is initiated and the final value of the stator voltage is limited by the magnetic saturation in the machine. The machine is then called SEIG and is capable to operate as a generator in isolation [13].

2.11.1.4 Operation problem of the SEIG system

The main operational problem of the SEIG system is its poor voltage and frequency regulation under varying load conditions. A change in the load impedance directly affects the machine excitation. This is because the reactive power of the excitation capacitors is shared by both the induction machine and the load impedance. Therefore, the generator's voltage drops when the load impedance is increased resulting in poor voltage regulation. On the other hand, the slip of the induction generator increases with increasing load, resulting in a load dependent frequency, even if the speed of the prime mover remains constant.

Many studies have been conducted in the past to regulate the voltage and frequency of a SEIG system operating with variable loads. A high cost speed govern is generally used as a conventional SEIG controller [12].

2.12 Power Electronics used in wind power generation system

power electronic converters are family electrical circuits which convert electrical energy from one level of voltage ,current ,or frequency to anther using power switching components .in all power converter families, energy conversion is function of different switching states. The process of switching the power devices in power converter topologies from one state to another is called modulation. Regarding different applications, various families of power converters with optimum modulation technique should be used to deliver the desired electrical energy to tale load with maximum efficiency and minimum cost. Three main families of power converters which are usually used in renewable energy system are [13].

- AC-DC converters
- DC-DC converters
- DC-AC converters

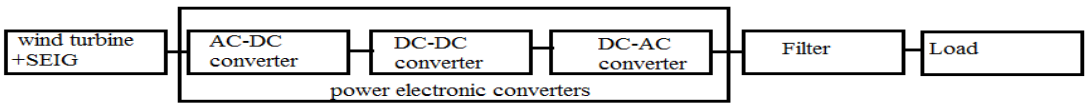

Figure (2.9): Families of power converters categorized according to their energy conversion in renewable energy system

2.12.1 AC-DC converters

A three phase low frequency rectifier is depicted in figure (2.10). Is converter operates at line frequency, so that the switching happens at 50Hz or 60Hz.Low frequency rectifiers are made up by diode or thyristor to change the AC voltage to DC voltage. However, rectifiers based on thyristors have freedom to change the firing angle to switch the thyristors , so that the amount of output DC voltage is controlled compared with diode rectifier. Using capacitor at output can increase the quality of the output voltage.

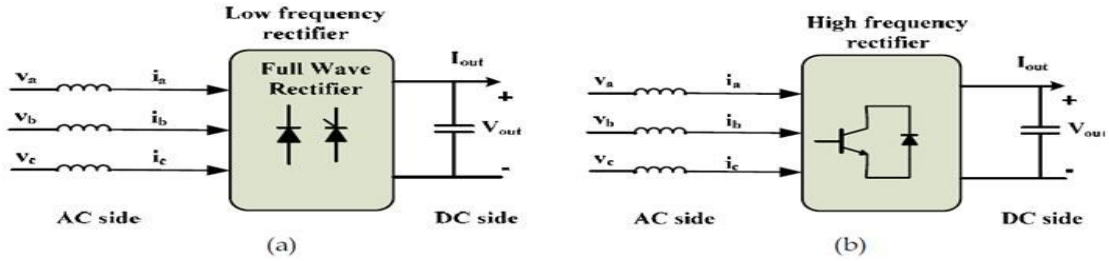

Figure (2.10): AC-DC converter (a) low frequency (b) high frequency

A three-phase controlled high frequency converter based on IGBT is show in figure (2.10) (b). This circuit can be change the input AC voltage into DC voltage. By controlling the duty cycle of the switches based on different modulation technique, the amount of output DC voltage can be controlled. Since the switches drive in high frequency the amount of harmonic content in current waveform is decreased. In addition, this configuration can provide bidirectional power flow between load and source [13].

2.12.2 DC-DC converter

DC-DC converters are a kind of high frequency converters which convert variable DC voltage to fixed DC voltage. Since the output voltage of renewable energy systems or rectifier convert is basically unregulated DC voltage, DC-DC converters are necessary to adjust the Dc voltage for different applications. Three basic in a buck converter the output voltage is normally less than input voltage. However, a boost converter has the ability to increase the input voltage base on duty cycle of the switch. A buck-boost converter can either buck or boost the input voltage. A boost converter is usually applied in renewable energy systems as the output voltage of these systems is low and unregulated [13].

2.12.3 DC-AC converter

This converter chop's the input DC voltage and generates an Ac voltage with desired magnitude and frequency with respect to the pulse patterns and modulation techniques [13].

2.13 Pitch control system design

Pitch control means that the blades can pivot upon their own longitudinal axis. The pitch control used for speed control, optimization of power production and to start and step the turbine, the control system structure used to generate the pitch angle reference is given in Figure (2.11). The pitch controller consists of two paths a nonlinear feed forward path, which generates β_0 and a linear feedback path, which generates $\Delta\beta$ [11].

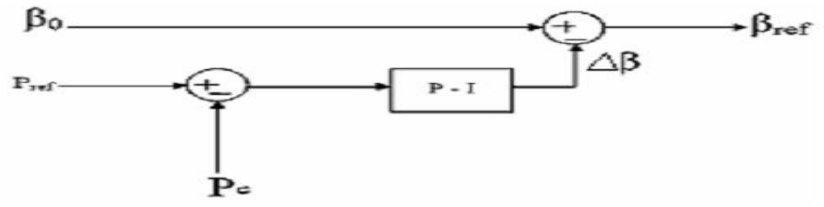

Figure (2.11) Pitch angle reference generator

The feed forward path uses the information about the desire power output, wind velocity and the turbine speed to determine the pitch angle required. Equation (2.5) gives the pitch angle as a function of the measured variables.

$$\beta_0 = \sqrt{\frac{1}{0.022}\left[\gamma - 5.6 - \frac{2P_{ref}e^{0.17\gamma}}{P_w}\right]} \qquad (2.5)$$

However, the feed forward term assumes that all the components are ideal and does not account for the losses in the system. The feedback path compensates for the losses by decreasing the pitch angle, if the output power is less than the desired power; to increase the power captured [11].

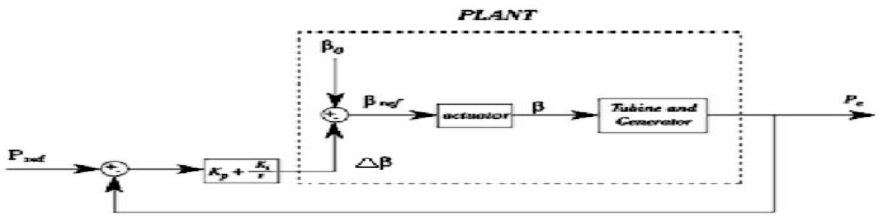

Figure (2.12) Plant and controller definition

- **Tuning Methods of PI and PID controllers:**

The PID controller tuning methods are classified into two main categories

1. Closed loop methods
2. Open loop methods

Closed loop tuning techniques refer to methods that tune the controller during automatic state in which the plant is operating in closed loop. The open loop techniques refer to methods that tune the controller when it is in manual state and the plant operates in open loop.

❖ The closed loop methods considered for simulation are:

- Ziegler-Nichols method
- Modified Ziegler-Nichols method
- Tyreus-Luyben method

❖ Open loop methods are:

- Open loop Ziegler-Nichols method
- C-H-R method
- Cohen and Coon method

Before proceeding with a brief discussion of these methods it is important to note that the non-interacting PID controller transfer function is:

$$G_c(s) = K_c(1 + \frac{t_1}{s} + t_I.s) \qquad (2.6)$$

Where:

k_c= proportional gain ,τ_I= Integral time , τ_D= derivative time

- **Closed Loop Zeigler - Nicholas**

This method is a trial and error tuning method based on sustained oscillations that was first proposed by Ziegler and Nichols (1942) This method that is probably the most known and the most widely used method for tuning of PID controllers is also known as online or continuous cycling or ultimate gain tuning method.

Having the ultimate gain and frequency (K_u and P_u) and using Table (2.1).

Table (2.1) Controller parameters for closed loop Ziegler-Nichols method

Controller	K_P	K_I	K_D
P	$0.5K_{CU}$	-	-
PI	$0.45K_{CU}$	$1.2K_P/T_U$	-
PID	$0.6K_{CU}$	$2K_P/T_U$	$K_PT_U/8$

- The disadvantages of this technique are:

-It is time consuming because a trial and error procedure must be performed

-It forces the process into a condition of marginal stability that may lead to unstable operation or a hazardous situation due to set point changes or external disturbances.

-This method is not applicable for processes that are open loop unstable.

-Some simple processes do not have ultimate gain such as first order and second order processes without dead time.

Step 1: Determine the sign of process gain (e.g. open loop test as in Cohen-Coon).

Step 2: Implement a proportional control and introducing a new set-point.

Step 3: Increase proportional gain until sustained periodic oscillation.

Step 4: Record ultimate gain and ultimate period: (K_U and T_U).

Step 5: Evaluate control parameters as prescribed by Ziegler and Nichols

CHAPTER THREE

MATHEMATICAL MODEL

3.1 Introduction

There are two common types of interfaces between SEIG and the load. The first configuration is designed as back-to-back PWM converter, the second configuration is a single switch mode rectifier and an inverter; the former is commonly considered as the technical ultimate operation but may be more expensive and complex, it has a lot of switches which cause more losses and voltage stress in addition to presence of Electromagnetic Interface (EMI), is usually used in the stand-alone or small scale wind farms for its simple topology and control, and most importantly, low cost [2].

There are many remote communities throughout the world where the electricity grid is not available. These communities are supplied with conventional energy sources. As it is well known, these conventional sources are very expensive and go to depletion. If these communities are affluent in wind energy, in this case, stand-alone wind energy systems can be considered as an effective way to supply power to the loads in these communities. It is one of the practicalities for self-sufficient power generation which involves using a wind turbine with battery storage system to create a stand-alone system for isolated communities located far from a utility grid. Load side voltage source inverter is responsible to supply controlled output load voltage in terms of amplitude and frequency to the load Wind energy supply systems are among the most interesting, low cost, and environmental friendly for supply power to remote communities which are affluent in wind energy resource.

3.2 Stand-Alone Wind Energy Supply System

The power circuit topology of the proposed variable speed stand-alone wind energy supply system is shown in Figure (3.1). The system consists of the following components:

- Variable speed Wind turbine.
- Self-exited induction generator (SEIG), driven by the wind turbine with using a gearbox.

- A single switch three phase mode rectifier which consists of a three phase diode bridge rectifier
- DC-DC boost converter.
- Batteries bank is connected to the DC-link voltage.
- A three phase voltage source inverter connected to the load through LC filter. The proposed model has been modeled and simulated using MATLAB/SIMULINK software program.

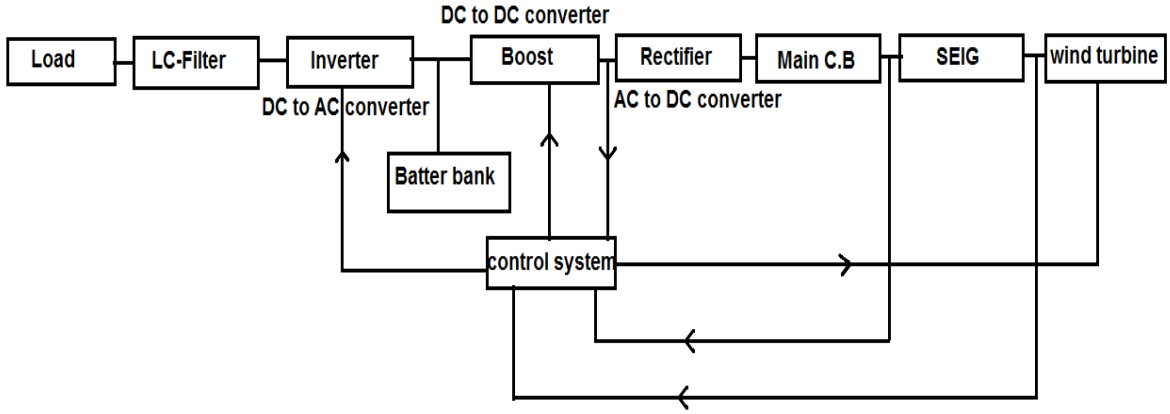

Figure (3.1): Power circuit topology of a variable speed stand-alone wind energy supply system.

3.3 Wind Turbine Model

Many wind turbines are equipped with fixed frequency induction generators. Thus the power generated is not optimized for all wind conditions. To operate a wind turbine at its optimum at different wind speeds, the wind turbine should be operated at its maximum power coefficient (Cp-optimum = 0.3-0.5). To operate around its maximum power coefficient, the wind turbine should be operated at a constant tip-speed ratio, which is proportional to ratio of the rotor speed to the wind speed. As the wind speed increases, the rotor speed should follow the variation of the wind speed. In general, the load to the wind turbine is regulated as a cube function of the rotor rpm to operate the wind turbine at the optimum efficiency. The aerodynamic power generated by wind turbine can be written as: [14].

$$P_m = 0.5\pi\rho R^2 V_w^3 C_p(\beta,\lambda) \qquad (3.1)$$

Where the aerodynamic power is expressed as a function of the specific density (ρ) of the air, the swept area of the blades (A) and the wind speed (V_w), to operate the wind turbine at its optimum efficiency (Cp-optimum), the rotor speed must be varied in the same proportion as the wind-speed variation. If we can track the wind speed precisely, the power can also be expressed in terms of the rotor speed [14].

$$P_m = K_P W^3 \tag{3.2}$$

Where:

$K_P \equiv \text{constant , equal } \frac{0.5\rho A R^5 C_p}{\lambda^3}$

$\omega \equiv$ angler speed

The power described by equation [3.2] will be called P_{ideal}.

The power coefficient C_p as a function of Tip-Speed Ratio (TSR) λ, where, λ is given in terms of rotor speed, ω(rad/sec), wind speed, V_w(m/s), and rotor radius, R (m) as

$$\lambda = \frac{R\omega}{V} \tag{3.3}$$

Wind turbine power coefficient, C_p is dependent upon λ. If pitch angle, β,is incorporated, C_p becomes a function of λ and

$$C_p(\beta,\lambda) = 0.5176\left[\frac{116}{\lambda_i} - 0.4 \times \beta - 5\right] e^{-\frac{21}{\lambda_i}} + 0.0068 \times \lambda_i \tag{3.4}$$

Where:

$$\frac{1}{\lambda_i} = \left[\frac{1}{[\lambda - 0.08\beta]}\right] - \left[\frac{0.035}{\beta^3+1}\right] \tag{3.5}$$

When the wind speed is increased the maximum power extracted from the wind is increased for the same turbine speed. The equations of the torque of the wind turbine are.

$$T_m = \frac{P_m}{\omega} \tag{3.6}$$

$$\frac{T_m - T_{shaft}}{2H} = \frac{dw}{dt} \tag{3.7}$$

Where: $T_{m=}$ mechanical torque, T_{shaft} =shaft torque, H=Inertia constant, p_m= mechanical power and $\frac{dw}{dt}$ is the differential of Turbine rotor speed.

- **Maximum Power Tracking Concept:**

The equations of the wind turbine mechanical power and mechanical torque were given in equations (3.1) and (3.6)). The wind turbine mechanical output power, P_m is affected by the ratio of the turbine shaft speed and the wind velocity, i.e., tip-speed-ratio ($\lambda=R\ \omega/V_w$). As a result of variations in wind velocity, the turbine shaft speed ω (or generator shaft speed ω_g), and wind turbine power P_m will change. Figure (3.2) shows a family of typical P_m versus ω curves for different wind velocities for system. As seen in this figure, different power curves have different maximum power, P_{max} (or optimal power, P_{opt}) [15].

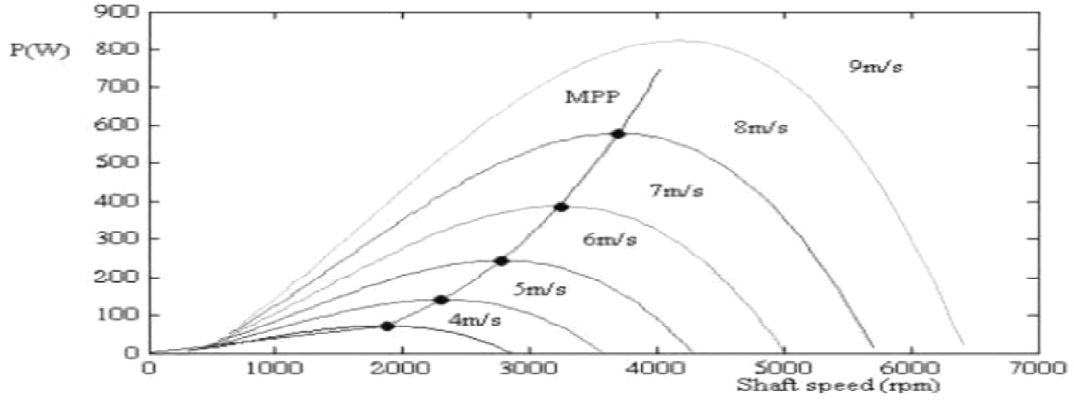

Figure (3.2): Wind turbine mechanical output power versus shaft speed

From mechanical design point of view, wind turbines are designed to operate at maximum power for an average wind speed. However, it is clear that wind speed dose not stay at an average level all the time. At lower wind speeds, tip speed ratio (λ) is increased (with constant rotor speed), and accordingly, the power coefficient C_p decreases (equation (3.4)). As a consequence, the wind turbine is not operating under optimal conditions (where C_p is low) most of the time. Optimal operating conditions can be achieved by employing a MPPT method. Implementing a

MPPT method depends on wind turbine structure [15].

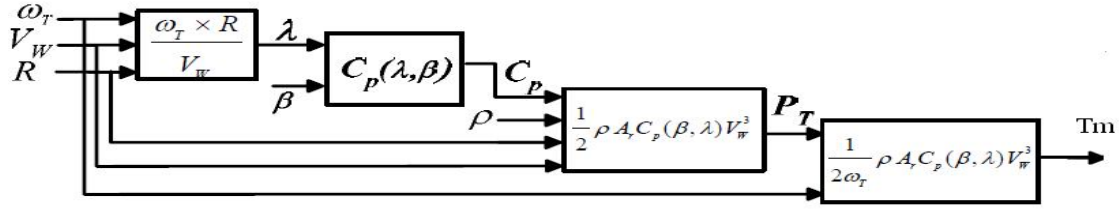

Figure (3.3) represent the wind turbine model.

3.4 Modeling of gear:

The mechanical system of the wind turbines plays a big role in the energy transformation. Most of the simple wind turbine gear box consists of two main shafts, the low speed shaft which is basically connected with the wind turbine blades, and the second one which is called the high speed shaft connected directly to the generator as shown in figure (3.4)

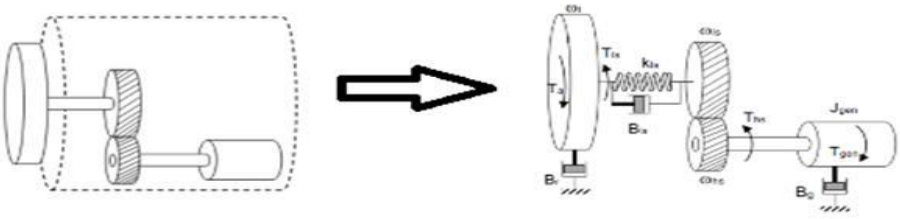

Figure (3.4): Typical gear of wind turbine

By applying Newton's second law for rotation system or using energy principles on the rotor, the mathematical model will be:

$$J_r W_t + B_r W_t - T_a - T_{ls} \qquad (3.8)$$

Where: J_r = rotor moment of inertia, $\dot{W}_t$ = rotor angular speed, B_r = rotor damping effect, T_a=applied torque on the rotor, T_{ls} =low speed shaft torque.

Whereas the same technique is applied for the driving gear, which basically its moment of inertia is cancelled, this will yield:

$$T_{ls} = J_{ls} W_t + B_{ls}(W_t - W_{ls}) + K_{ls}(\theta_t - \theta_{ls}) \qquad (3.9)$$

Where:

J_{ls} =driver moment of inertia (cancelled), W_{ls} =angular speed of the low speed shaft, K_{ls}=stiffness of low speed shaft, θ_t = rotor angular displacement, θ_{ls}= low speed angular displacement.

Since the moment of inertia of gear one is considered, and then the mathematical model of it is calculated as

$$T_{G1} = J_{G1} W_{ls} + B_{ls} W_{ls} + K_{ls}(\theta_{ls} - \theta_t) \qquad (3.10)$$

Whereas for gear 2, the dynamic equation is written as:

$$T_{sh} = J_{G2} W_{hs} + B_G W_{ls} + K_{hs}(\theta_{hs} - \theta_G) \qquad (3.11)$$

3.5 Induction machine Model

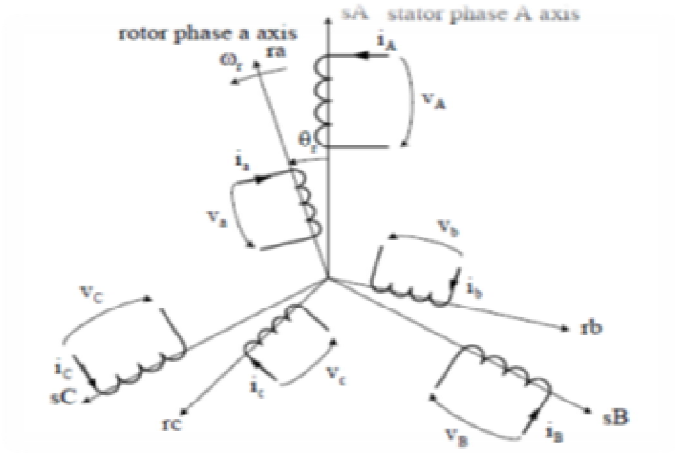

Figure (3.5): Three phase induction machine

The voltages equations of three phase induction machine are:

$$[V]=[R]\cdot[I]+\frac{d[\psi]}{dt} \tag{3.12}$$

$$[\psi]=[L]\cdot[I] \tag{3.13}$$

Where:

- $[V]=[V_A\ V_B\ V_C\ V_a\ V_b\ V_c]^t \rightarrow$ are the voltages applied to each stator and rotor phases.
- $[I]=[I_A\ I_B\ I_C\ I_a\ I_b\ I_c]^t \rightarrow$ are the currents in each stator and rotor phases.
- $[\psi]=[\varphi_A\ \varphi_B\ \varphi_C\ \varphi_a\ \varphi_b\ \varphi_c]^t \rightarrow$ are the fluxes linked with each stator and rotor.
- $[R]$ is the resistance matrix and $[L]$is the inductance matrix.

The inductance and resistance matrix are defind as:

$$[L]=\begin{bmatrix} L_s & -0.5M_S & -0.5M_S & M_{sr}f_1 & M_{sr}f_2 & M_{sr}f_3 \\ -0.5M_S & L_s & -0.5M_S & M_{sr}f_3 & M_{sr}f_1 & M_{sr}f_2 \\ -0.5M_S & -0.5M_S & L_s & M_{sr}f_2 & M_{sr}f_3 & M_{sr}f_1 \\ M_{sr}f_1 & M_{sr}f_3 & M_{sr}f_2 & L_r & -0.5M_r & -0.5M_r \\ M_{sr}f_2 & M_{sr}f_1 & M_{sr}f_3 & -0.5M_r & L_r & -0.5M_r \\ M_{sr}f_3 & M_{sr}f_2 & M_{sr}f_1 & -0.5M_r & -0.5M_r & L_r \end{bmatrix} \tag{3.14}$$

$$[R]=\begin{bmatrix} R_s & 0 & 0 & 0 & 0 & 0 \\ 0 & R_s & 0 & 0 & 0 & 0 \\ 0 & 0 & R_s & 0 & 0 & 0 \\ 0 & 0 & 0 & R_r & 0 & 0 \\ 0 & 0 & 0 & 0 & R_r & 0 \\ 0 & 0 & 0 & 0 & 0 & R_r \end{bmatrix} \tag{3.15}$$

where:

$L_s = L_{\sigma s} + M_s \rightarrow$ stator self-inductance

$L_r = L_{\sigma r} + 1.5M_r \rightarrow$ rotor self-inductance

$L_{\sigma s}, L_{\sigma r} \rightarrow$ stator and rotor leakage indactance

$M_s, M_r \rightarrow$ stator and rotor mutual indactance

$M_{sr} \rightarrow$ stator-rotor mutual inductance

The coefficients f_1, f_2, f_3

$$f_1 = \cos\theta_r \ , f_2 = \cos\left(\theta_r + \frac{2\pi}{3}\right), f_3 = \cos\left(\theta_r - \frac{2\pi}{3}\right) \tag{3.16}$$

All these in inductances can easily be measured a wound rotor induction machine. For squirrel-cage induction machines, these inductances can normally be estimated from no-load and locked rotor tests. Referring the rotor parameters to stator the inductances become equals:

$$M_s = M_r = M_{sr} \tag{3.17}$$

The impudence matrix is defined as:

$$[Z]=\begin{bmatrix} R_s+L_sP & -0.5PM_S & -0.5PM_S & M_{sr}Pf_1 & M_{sr}Pf_2 & M_{sr}Pf_3 \\ -0.5PM_S & R_s+L_sP & -0.5PM_S & M_{sr}Pf_3 & M_{sr}Pf_1 & M_{sr}Pf_2 \\ -0.5PM_S & -0.5PM_S & R_s+L_sP & M_{sr}Pf_2 & M_{sr}Pf_3 & M_{sr}Pf_1 \\ M_{sr}Pf_1 & M_{sr}Pf_3 & M_{sr}Pf_2 & R_r+L_rP & -0.5PM_r & -0.5PM_r \\ M_{sr}Pf_2 & M_{sr}Pf_1 & M_{sr}Pf_3 & -0.5PM_r & R_r+L_rP & -0.5PM_r \\ M_{sr}Pf_3 & M_{sr}Pf_2 & M_{sr}Pf_1 & -0.5PM_r & -0.5PM_r & R_r+L_rP \end{bmatrix} \tag{3.18}$$

The transformation of the 3-phase induction machine to two phase machine is done by using the phase transformation matrix C_1 and commutater transformation C_2 as follows:

$$C_1 = \sqrt{\frac{2}{3}} \begin{Vmatrix} \frac{1}{\sqrt{2}} & 1 & 0 \\ \frac{1}{\sqrt{2}} & -\frac{1}{2} & \frac{\sqrt{3}}{2} \\ \frac{1}{\sqrt{2}} & -\frac{1}{2} & -\frac{\sqrt{3}}{2} \end{Vmatrix} \tag{3.19}$$

$$C_2 = \begin{Vmatrix} \sin\theta & \cos\theta \\ \cos\theta & -\sin\theta \end{Vmatrix} \tag{3.20}$$

✓ **The stator is not requires a transformation by C_2**

The new impedance matrix after applied C_1

$$[Z]' = \begin{bmatrix} R_s + L_s P & 0 & M\,P\cos\theta & M\,P\sin\theta \\ 0 & R_s + L_s P & M\,P\sin\theta & -M\,P\cos\theta \\ M\,P\cos\theta & M\,P\sin\theta & R_r + L_r P & 0 \\ M\,P\sin\theta & -M\,P\cos\theta & 0 & R_r + L_r P \end{bmatrix} \tag{3.21}$$

The new impedance matrix after applied C_2 to the rotor only

$$[Z]'' = \begin{bmatrix} R_s + L_s P & M\,P & 0 & 0 \\ M\,P & R_r + L_r P & \omega_m M & \omega_m L_r \\ 0 & 0 & R_s + L_s P & MP \\ -\omega_m M & -\omega_m L_r & MP & R_r + L_r P \end{bmatrix} \tag{3.22}$$

The voltages and currents equations after transformation when applied C_{12} to the rotor voltage and applied C_1 to the stator

$$[V]'' = \begin{bmatrix} V_D \\ V_d \\ V_Q \\ V_q \end{bmatrix} \tag{3.23}$$

$$[I]'' = \begin{bmatrix} I_D \\ I_d \\ I_Q \\ I_q \end{bmatrix} \tag{3.24}$$

The new voltage equation of the induction machine in dq-model:

$$\begin{bmatrix} V_D \\ V_d \\ V_Q \\ V_q \end{bmatrix} = \begin{bmatrix} R_s + L_s P & M P & 0 & 0 \\ M P & R_r + L_r P & \omega_m M & \omega_m L_r \\ 0 & 0 & R_s + L_s P & MP \\ -\omega_m M & -\omega_m L_r & MP & R_r + L_r P \end{bmatrix} \begin{bmatrix} I_D \\ I_d \\ I_Q \\ I_q \end{bmatrix} \quad (3.25)$$

3.6 Modeling of Self-Excited Induction Generator

Figure (3.6) (a) & (b) depict the d-q axis equivalent circuit of SEIG with capacitor connected across the stator windings of the generator. Using Kirchoff's voltage the loop equations (3.26)-(3.29) of the SEIG equivalent circuit are written as [16].

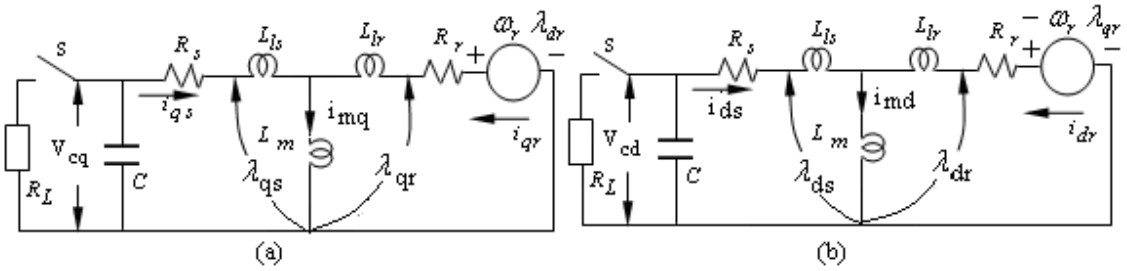

Figure (3.6) D-Q Equivalent circuit of self-excited induction generator with load

$$R_s i_{qs} + L_{ls} \frac{di_{qs}}{dt} + L_m \frac{di_{qr}}{dt} + \frac{1}{C} \frac{di_{qs}}{dt} = V_{cq} \quad (3.26)$$

$$R_r i_{qr} + L_{lr} \frac{di_{qr}}{dt} + L_m \frac{di_{qs}}{dt} + \frac{1}{C} \frac{di_{qr}}{dt} = \omega_r \lambda_{dr} \quad (3.27)$$

$$R_s i_{qs} + L_{ls} \frac{di_{qs}}{dt} + L_m \frac{di_{qr}}{dt} + \frac{1}{C} \frac{di_{qs}}{dt} = -V_{cd} \quad (3.28)$$

$$R_r i_{qr} + L_{lr} \frac{di_{qr}}{dt} + L_m \frac{di_{qs}}{dt} + \frac{1}{C} \frac{di_{qr}}{dt} = -\omega_r \lambda_{qr} \quad (3.29)$$

$$[C] = [Z] \times [I] + [V] \quad (3.30)$$

Where:

$$[C] = [0 \quad 0 \quad 0 \quad 0]^t, , [V] = \begin{bmatrix} V_{cq} & V_{cd} & K_q & K_d \end{bmatrix}^t, , [I] = \begin{bmatrix} i_{qs} & i_{ds} & i_{qr} & i_{dr} \end{bmatrix}^t$$

Where:

- $[V]=\left[V_{cq}\ V_{cd}\right]$ instantaneous direct and quadrature axis voltage(V).
- $[I]=\left[I_{qs}\ I_{ds}\ I_{qr}\ I_{dr}\right]^{t}$ instantaneous stator and rotor direct and quadrature axis current(A).
- $\left[K_q\ K_d\right]$ direct and quadrature axis constant.

And :

$$[Z]=\begin{bmatrix} R_s+PL_{ls}+\dfrac{1}{PC} & 0 & PL_m & 0 \\ 0 & R_s+PL_{ls}+\dfrac{1}{PC} & 0 & PL_m \\ PL_m & -\omega_r L_m & R_r+PL_{lr} & -\omega_r L_m \\ \omega_r L_m & PL_m & -\omega_r L_m & R_r+PL_{lr} \end{bmatrix} \quad (3.31)$$

Where, p is equal to d/dt in the matrix [Z]

The equation (3.31) describes the dynamic characteristics behavior of SEIG in matrix form. Owing to the magnetic saturation of SEIG stator core, its behavior is non-linear. The magnetizing current is to be updated in each step of integration. Therefore, the new magnitude of the magnetizing current i_m is obtained using the equation (3.32),

$$|i_m|=\sqrt{\left(i_{qs}+i_{qr}\right)^2+\left(i_{ds}+i_{dr}\right)^2} \quad (3.32)$$

Hence, the magnitude of the generated air gap voltage of SEIG in the steady state is given by

$$E_g=\omega_r L_m|i_m| \quad (3.33)$$

It is noted that L_m is not a constant but a function of the magnetizing current i_m and can be expressed as

$$L_m=f_m|i_m| \quad (3.34)$$

This dependency is determined by a synchronous impedance test. The developed electromagnetic torque and the torque balance equations are [3.35] & [3.36]:

$$T_e=\left(\frac{2}{3}\right)\left(\frac{P}{2}\right)L_m\left(i_{dr}i_{qs}-i_{qr}i_{ds}\right) \quad (3.35)$$

$$T_{shaft}=T_e+J\left(\frac{2}{P}\right)P\omega_r \quad (3.36)$$

The torque balance equation can be expressed in speed derivative form as

$$P\omega_r\left(\frac{P}{2J}\right)=T_e-T_{shaft} \quad (3.37)$$

The generated phase voltage and stator currents are derived from d-q axes values using the equations (3.38) & (3.39)

$$\begin{bmatrix} V_a = V_1\cos\theta_1 + V_2\sin\theta_1 \\ V_b = V_1\cos(\theta_1-\omega_1) + V_2\sin(\theta_1-\omega_1) \\ V_c = V_1\cos(\theta_1+\omega_1) + V_2\sin(\theta_1+\omega_1) \end{bmatrix} \quad (3.38)$$

$$\begin{bmatrix} i_a = I_1\cos\theta_1 + I_2\sin\theta_1 \\ i_b = I_1\cos(\theta_1-\omega_1) + I_2\sin(\theta_1-\omega_1) \\ i_c = I_1\cos(\theta_1+\omega_1) + I_2\sin(\theta_1+\omega_1) \end{bmatrix} \quad (3.39)$$

Where:

$$\begin{bmatrix} V_1 = V_{qs}\cos\theta + V_{ds}\sin\theta \\ V_2 = -V_{qs}\sin\theta + V_{ds}\cos\theta \end{bmatrix} \quad (3.40)$$

$$\begin{bmatrix} I_1 = I_{qs}\cos\theta + I_{ds}\sin\theta \\ I_2 = -I_{qs}\sin\theta + I_{ds}\cos\theta \end{bmatrix} \quad (3.41)$$

$$\begin{bmatrix} \omega_1 = \dfrac{2\pi}{3} \\ \theta = \omega_e t \\ \theta_1 = 0 \end{bmatrix} \quad (3.42)$$

3.7 Mathematical Model of DC/DC Converter

The standard unidirectional topology of the DC/DC boost converter (also known as step-up converter or chopper) consist of a switching-mode power device containing basically two semiconductor switches (a rectifier diode and a power transistor with its corresponding anti-parallel diode) and two energy storage devices (an inductor and a smoothing capacitor) for producing an output DC voltage at a level greater than its input dc voltage. This converter acts as an interface between the full-wave rectifier bridge and the VSI, by employing pulse-width modulation (PWM) control techniques. Operation of the DC/DC converter in the continuous (current) conduction mode (CCM), i.e. the current flowing continuously in the inductor during the entire switching cycle, makes simple the development of the state-space model because only two switch states are possible during a switching cycle, namely, (i) the power switch T_b is on and the diode D_b is off; or (ii) T_b is off and D_b is on. In steady-state CCM operation and neglecting

parasitic components, the state space equation that describes the dynamics of the DC/DC boost converter is given by equation (3.43)

$$\begin{bmatrix} SI_L \\ SV_d \end{bmatrix} = \begin{bmatrix} 0 & \frac{1-S_{dc}}{L} \\ -\frac{1-S_{dc}}{C} & 0 \end{bmatrix} \begin{bmatrix} I_L \\ V_d \end{bmatrix} + \begin{bmatrix} \frac{1}{L} & 0 \\ 0 & -\frac{1}{C} \end{bmatrix} \begin{bmatrix} V_g \\ I_d \end{bmatrix} \tag{3.43}$$

Where:

I_L: chopper input current (inductor current).

V_g: chopper input voltage, the same as the three-phase rectifier output voltage.

V_d: chopper output voltage, coinciding with the inverter DC bus voltage.

i_d: chopper output current.

S_{dc}: switching function of the boost DC/DC converter. The switching function S_{dc} of the power converter is a two-leveled waveform characterizing the signal that drives the power switch Tb of the DC/DC boost converter, defined as follows:

$$S_{dc} = \begin{Bmatrix} 0, \text{for the switch } T_b \text{ off} \\ 1, \text{ for the switch } T_b \text{ on} \end{Bmatrix} \tag{3.44}$$

If the switching frequency of the power switches is significantly higher than the natural frequencies of the DC/DC converter, this discontinuous model can be approximated by a continuous state-space averaged (SSA) model, where a new variable D is introduced. In the (0 to 1) interval, D is a continuous function and represents the modulation index of the DC/DC converter, defined as the ratio of time during which the power switch Tb is turned-on to the period of one complete switching cycle, Ts. This variable is used for replacing the switching function in equation (4.44), yielding the following SSA expression:

$$\begin{bmatrix} SI_L \\ SV_d \end{bmatrix} = \begin{bmatrix} 0 & \frac{1-D}{L} \\ -\frac{1-D}{C} & 0 \end{bmatrix} \begin{bmatrix} I_L \\ V_d \end{bmatrix} + \begin{bmatrix} \frac{1}{L} & 0 \\ 0 & -\frac{1}{C} \end{bmatrix} \begin{bmatrix} V_g \\ I_d \end{bmatrix} \tag{3.45}$$

Since, in steady-state conditions the inductor current variation during both, on and off times of T_b are essentially equal, so there is not net change of the inductor current from cycle to cycle, and assuming a constant DC output voltage of the boost converter, the steady-state input-to-output voltage conversion relationship of the boost converter is

easily derived from equation (3.45) by setting the inductor current derivative at zero, yielding equation (3.46) [12].

$$V_d = \frac{V_g}{1-D} \tag{3.46}$$

In the same way, the relationship between the average inductor current I_L and the DC/DC converter output current Id in the CCM can be derived, as follows:

$$I_d = (1-D)I_L \tag{3.47}$$

3.8 Mathematical of Voltage source inverter

The three-phase two level six pulse inverter proposed corresponds to a DC/AC switching power inverter using IGBTs operated through sinusoidal PWM.

The mathematical equations describing and representing the operation of the voltage source inverter can be derived .by taking into account some assumptions respect to its operating conditions. For this purpose, a simplified equivalent VSI connected to the electric load is considered, also referred to as an averaged model, which assumes the inverter operation under balanced conditions as ideal, i.e. the voltage source inverter is seen as an ideal sinusoidal voltage source operating at fundamental frequency. The high frequency harmonics produced by the inverter as result of the sinusoidal PWM control techniques are mostly filtered by the low pass sine wave filters and the net instantaneous output voltages at the point of common coupling resembles three sinusoidal waveforms phase-shifted 120º between each other. This ideal inverter is shunt-connected to the load an equivalent inductance L_s, and an equivalent series resistance R_s, and VSI semiconductors conduction losses. In the DC side, the equivalent capacitance of the one DC bus capacitor, C_d and where as the switching losses of the VSI and power losses in the DC capacitor is considered by a parallel resistance R_p. As a result, the dynamics equations governing the instantaneous values of the three-phase output voltages in the AC side of the VSI and the current exchanged with the load can be directly derived by as follows:

$$\begin{bmatrix} v_{inva} \\ v_{invb} \\ v_{invc} \end{bmatrix} = \left[R_S + SL_s\right] \begin{bmatrix} i_a \\ i_b \\ i_c \end{bmatrix} \tag{3.48}$$

Under the assumption that the system has no zero sequence components (operation under balanced conditions), all currents and voltages can be uniquely transformed into the synchronous-rotating orthogonal two-axes reference frame, in which each vector is described by means of its d and q components, instead of its three a, b, c components. Thus, the new coordinate system is defined with the d-axis always coincident with the instantaneous voltage vector.

Defining the d-axis to be always coincident with the instantaneous voltage vector v, yields v_d equals |v|, while v_q is null. Consequently, the d-axis current component contributes to the instantaneous active power and the q-axis current component represents the instantaneous reactive power. This operation permits to develop a simpler and more accurate dynamic model of the inverter. By applying Park's transformation stated by equation (3.49), equations (3.48) can be transformed into the synchronous rotating d-q reference frame as follows (equation (3.50)):[12].

$$K_s = \frac{2}{3}\begin{bmatrix} \cos\theta & \cos\left(\theta - \frac{2\pi}{3}\right) & \cos\left(\theta + \frac{2\pi}{3}\right) \\ -\sin\theta & -\sin\left(\theta - \frac{2\pi}{3}\right) & -\sin\left(\theta + \frac{2\pi}{3}\right) \\ \frac{1}{2} & \frac{1}{2} & \frac{1}{2} \end{bmatrix} \qquad (3.49)$$

With:

$\theta = \int_0^t \omega(t)dt + \theta(0)$ angle between the *d*-axis and the reference phase axis, and t: integration variable ω: synchronous angular speed of the network voltage at the fundamental system frequency

$$\begin{bmatrix} v_d \\ v_q \\ v_0 \end{bmatrix} = K_s \begin{bmatrix} v_{inva} \\ v_{invb} \\ v_{invc} \end{bmatrix} \quad \begin{bmatrix} i_d \\ i_q \\ i_0 \end{bmatrix} = K_s \begin{bmatrix} i_a \\ i_b \\ i_c \end{bmatrix} \qquad (3.50)$$

Then, by neglecting the zero sequence components, equations (3.48) and (3.50) are derived.

$$\begin{bmatrix} v_{invd} \\ \\ v_{invq} \end{bmatrix} = (R_s + sL_s)\begin{bmatrix} i_d \\ \\ i_q \end{bmatrix} + \begin{bmatrix} -\omega & 0 \\ 0 & \omega \end{bmatrix} L_s \begin{bmatrix} i_d \\ \\ i_q \end{bmatrix} \qquad (3.51)$$

The relation between the DC side voltage V_d and the generated AC voltage V_{inv} can be described through the average switching function matrix in the d-q reference frame $S_{av,dq}$

of the inverter, as given by equation (3.52). This relation assumes that the DC capacitors voltages are balanced and equal to V_d

$$\begin{bmatrix} v_{invd} \\ \\ v_{invq} \end{bmatrix} = S_{av,dq} V_d \tag{3.52}$$

$$S_{av,dq} = \begin{bmatrix} S_{avd} \\ \\ S_{avq} \end{bmatrix} = \frac{1}{2} m_i \begin{bmatrix} \cos\alpha \\ \sin\alpha \end{bmatrix} \tag{3.53}$$

Being, m_i: modulation index of the voltage source inverter, m_i = (0, 1) [12].

3.9 Mathematical model of three phase bridge rectifiers

The three-phase bridge rectifier is very common in high-power applications. It can operate with or without a transformer and gives six-pulse ripples on the output voltage. The diodes are numbered in order of conduction sequences and each one conducts for 120^o. The conduction sequence for diodes is 12, 23,34,45,56, and 61. The pair of diodes which are connected between that pair of supply lines having the highest amount of instantaneous line-to-line voltage will conduct. The line-to-line voltage is $\sqrt{3}$ times the phase voltage of a three-phase Y-connected source [1٧].

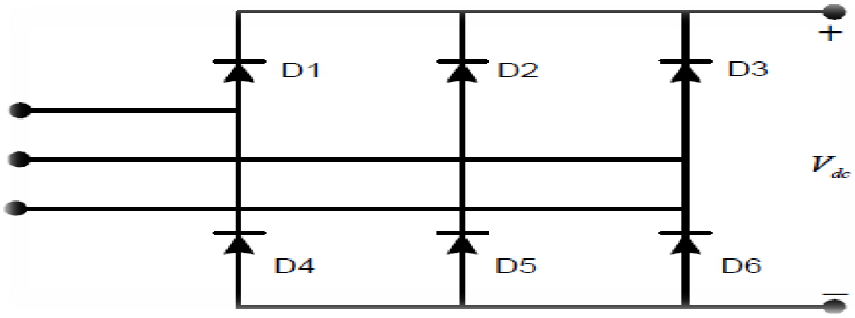

Figure (3.7) three phase full wave rectifier

$$V_{dc} = \frac{6}{2\pi} \int_{\frac{\pi}{3}}^{\frac{2\pi}{3}} \sqrt{3} V_m \sin\theta d\theta \tag{3.54}$$

$$V_{dc} = V_m \frac{3\sqrt{3}}{\pi} = 1.654 V_m \tag{3.55}$$

$$I_{dc} = V_m \frac{3\sqrt{3}}{\pi R} = 1.654 \frac{V_m}{R} \tag{3.56}$$

$$V_{rms} = \left[\frac{6}{2\pi} \int_{\frac{\pi}{3}}^{\frac{2\pi}{3}} (\sqrt{3} V_m \sin\theta)^2 d\theta \right]^{\frac{1}{2}} \quad (3.57)$$

$$V_{rms} = \left[\frac{3}{2} + \frac{9 \times \sqrt{3}}{4\pi} \right]^{\frac{1}{2}} V_m = 1.6554 V_m \quad (3.58)$$

$$I_{rms} = \left[\frac{3}{2} + \frac{9 \times \sqrt{3}}{4\pi} \right]^{\frac{1}{2}} \frac{V_m}{R} = 1.6554 \frac{V_m}{R} \quad (3.59)$$

The diode (r.m.s) current given by:

$$I_r = 1.6554 \frac{V_m}{\sqrt{3} R} = 0.9667 \frac{V_m}{R} = 0.7804 \frac{V_{L.L}}{R} \quad (3.60)$$

The rectifier line current given by:

$$I_S = 0.9667 \sqrt{2} \frac{V_m}{R} = 1.36712 \frac{V_m}{R} = 1.1036 \frac{V_{L.L}}{R} \quad (3.61)$$

CHAPTER FOUR

RESULTS AND DISCUSSIONS

4.1 Introduction

This chapter presents performance characteristics of variable speed wind turbine connected to self –excited induction generator (SEIG) fed current source inverter for isolated wind energy conversion system. The induction generator, solid state power electronic converter devices and inductor filter components are modeled by using MAT LAB / SIMULINK. The power electronic converters and pitch control based on power

signal feedback (PSF) method are used to obtain the maximum output power from the wind. The PID-controller results of the control pitch angle are compared with the PI-controller results. And the results are displayed. For the other case study for wind generation system, showing the importance of uninterrupted feeding system for electrical load

4.2 Maximum power point tracking (TMPP)

In this part the results of using two types of controllers PID-controller and PI-controller is presented. In order to assess the capability of the system in tracking maximum power point at varying wind velocity, a step change in the wind velocity is applied to the system figure (4.1). The system is first operating at the wind velocity of V_{w1}=8m/s from t=0sec to t= 2.5sec. The wind velocity is increased to 9m/s from t=2.5sec to t=5sec and the wind velocity is increased to 10 m/s from t=5sec to t=7.5sec.

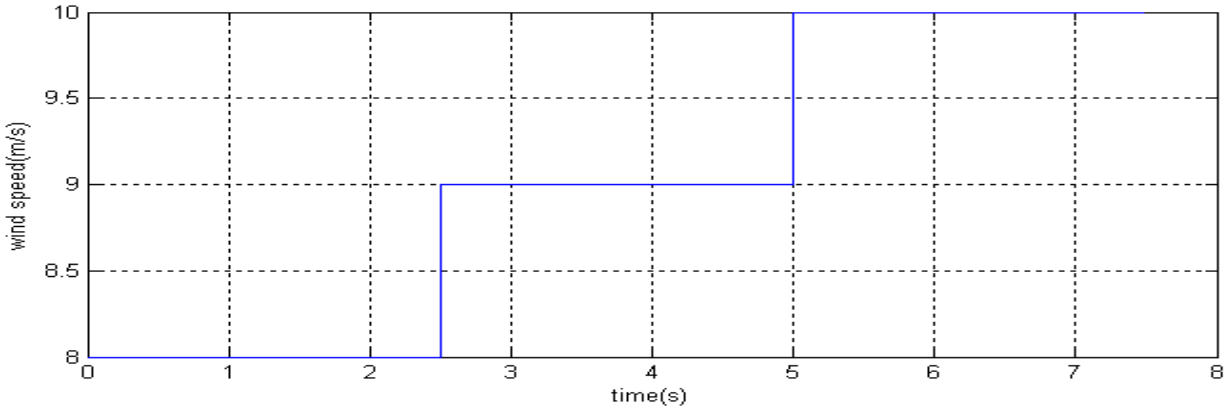

Figure (4.1) Wind speed

Figure (4.2) represent the power coefficient (C_P) with respect to the time, when using PID-controller, It is noticed from Figure (4.2) that the controller is able to search for maximum power and keep the power coefficient of the wind turbine is much closed.

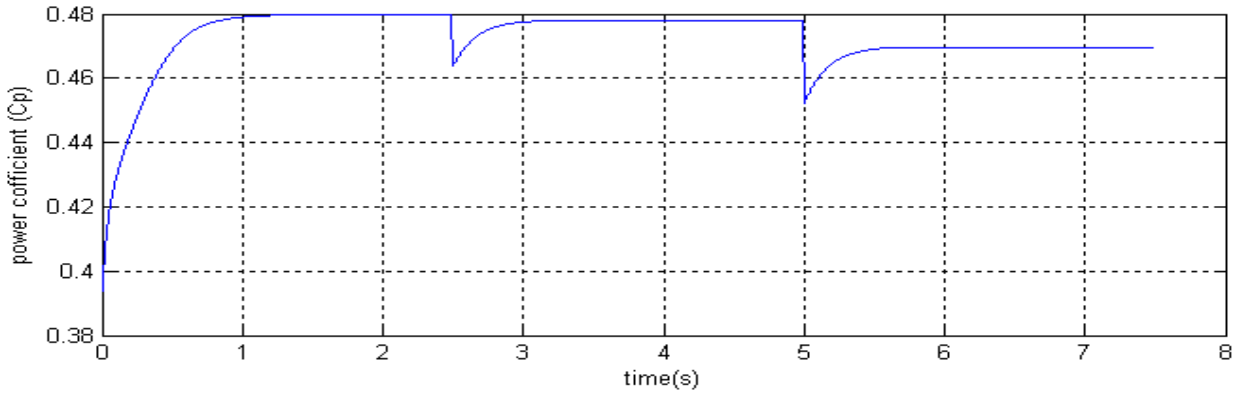

Figure (4.2) Power coefficient (Cp) with the PID-controller

Figure (4.3) shows the active power generated by SEIG when using PID-controller. The active power generated by the machine at wind speed 8m/s and excitation capacitance of 2VAR is 2865Watts and maintain the load as constant. The active power reached to steady state value at 1.8sec. If there is any increase in the wind speed than there is the active power is increased. The active power generated by the machine at wind speed is equal 9m/s is 3912W and reached to steady state value at 1seconds. The active power generated by the machine at rated wind speed (10m/s) is 5000W and reached to steady state value at 0.5sec.

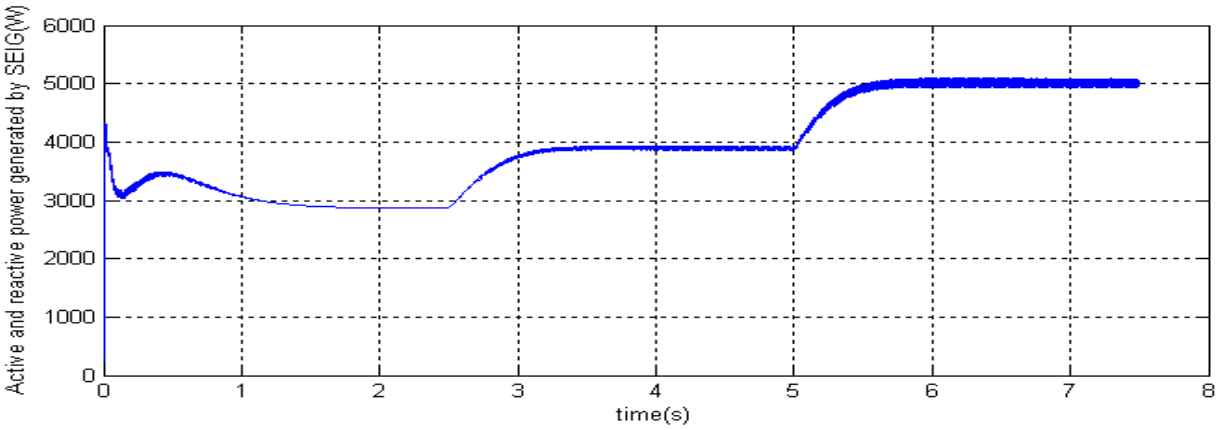

Figure (4.3) Active power generated by (SEIG) with the PID-controller

Figure (4. 4) represents a change in the speed of the generator when changing wind speed according to figure (4.1) as well as when the use of PID-controller. The speed of the generator is equal 0.81 P.u when the wind speed is equal 8 m/s. Note when increasing the wind speed increases the speed of the generator. When the wind speed has become 9m / s speed of the generator became 0.88pu.

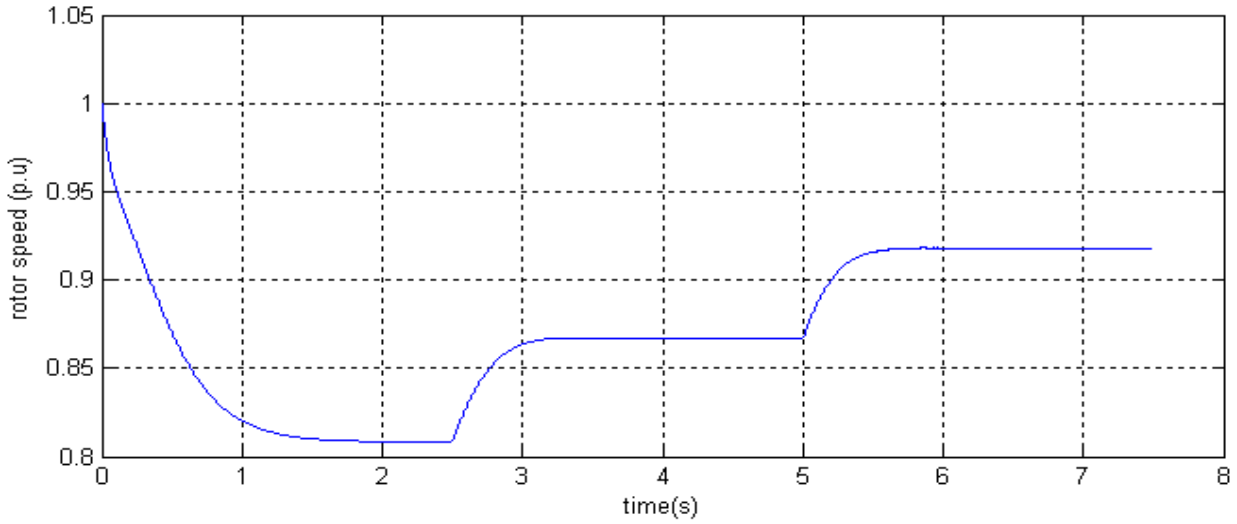

Figure (4.4) SEIG speed (p.u) with the PID-controller

Figure (4.5) shows the change in the Tip speed ration (λ) when used PID-controller. The optimal value of the wind turbine is equal 8.1. From the shape it starts from the highest value and then decline to settle at 8.1 when the wind speed 8m/s. Also note when the wind speed increased to 9m/s. the Tip speed ration at first declined and then increased again to settle at 7.8. And when the wind speed is equal rated value (10m/s) the Tip speed ratio settle at 7.49.

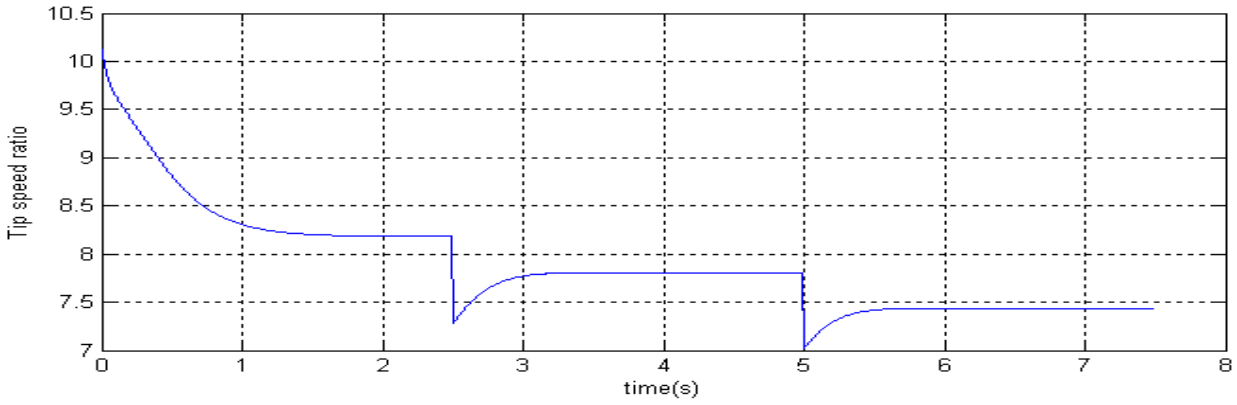

Figure (4.5) Tip speed ratio (λ) used PID-controller

Figure (4.5) shows the pitch angle of the wind turbine when used PID-controller. The optimal value of the pitch angle is equal 0. Note that the PID- controller keeps the optimum value during the period. So it is a good controller.

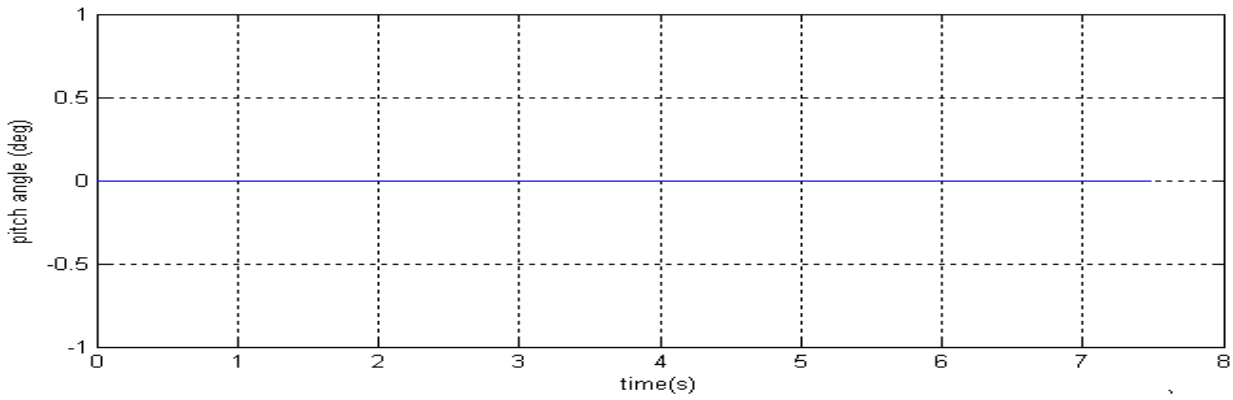

Figure (4.6) pitch angle with PID-controller

Figure (4.7) represent the power coefficient (C_P) with respect to the time, when using PI-controller, It is noticed from Figure (4.7) that the PI-controller is able to keep the power coefficient of the wind turbine is near to optimal value(0.48) . We note that the value of the power coefficient from the curve is begins with the small value then increases to settle at 0.479 when the wind speed is equal 8m/s. And when the wind speed increases the power coefficient is reduce at initially and then rise to settle at 0.476 when the wind speed is equal 9m/s.

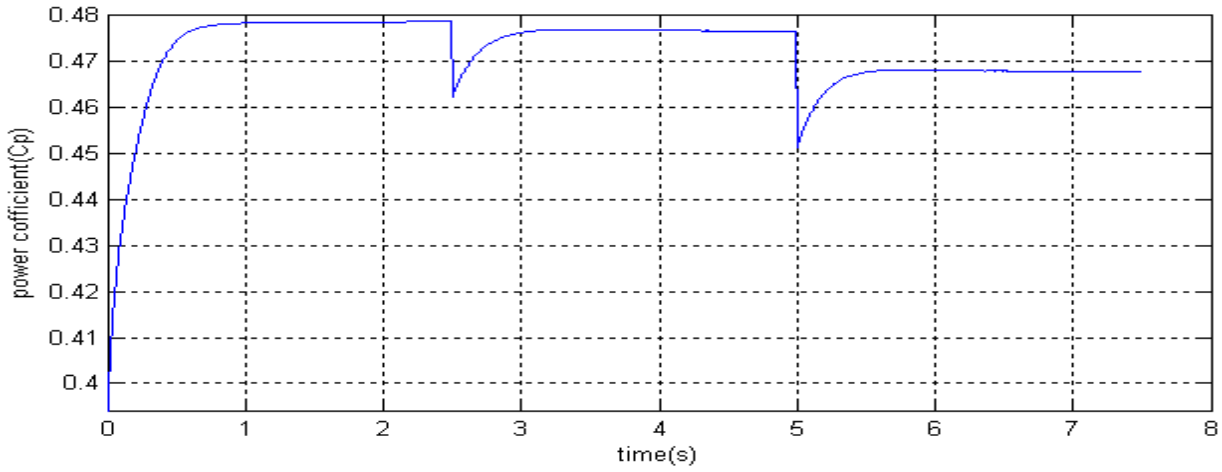

Figure (4.7) Power coefficient (Cp) with PI-controller

Figure (4.8) represents the power curve of the generator when the system is controlled by PI- controller. The basic observation is that the generated power depends on the change in wind speed. Thus the importance of the control system to maintain the value of the output power to the maximum value in a fixed amount, From the curve we observe that PI- controller is keep to the value of output power is equal 2818W when the wind speed

8m/s. Also note the increased output power with increased wind speed where output power is equal 3906W when the wind speed is equal 9m/s.

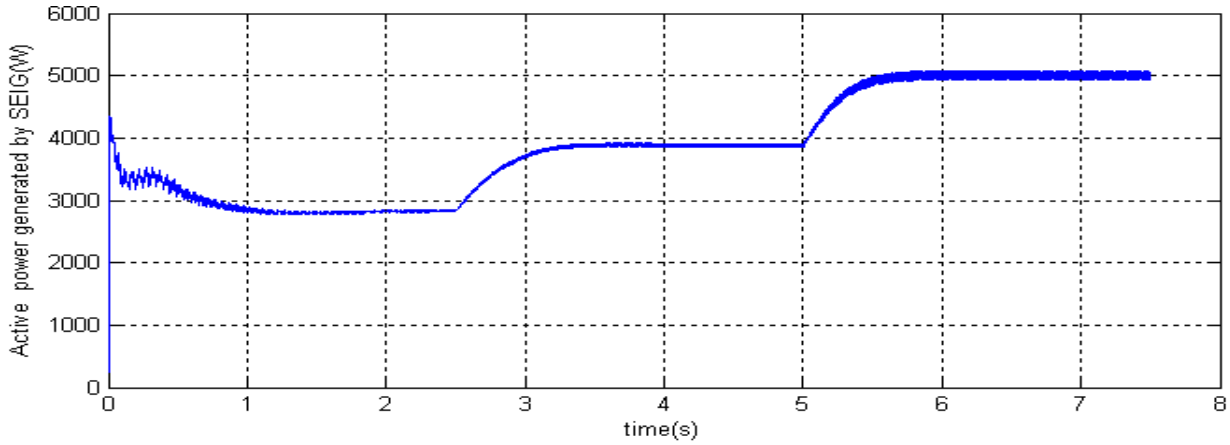

Figure (4.8) Active power generated by (SEIG) (W) using PI-controller

Figure (4.9) represents the change in speed of the generator when using PI-controller in control system for wind power generation system. from the curve note that the speed of the generator stabilizes at a time on a certain value for the change in wind speed.

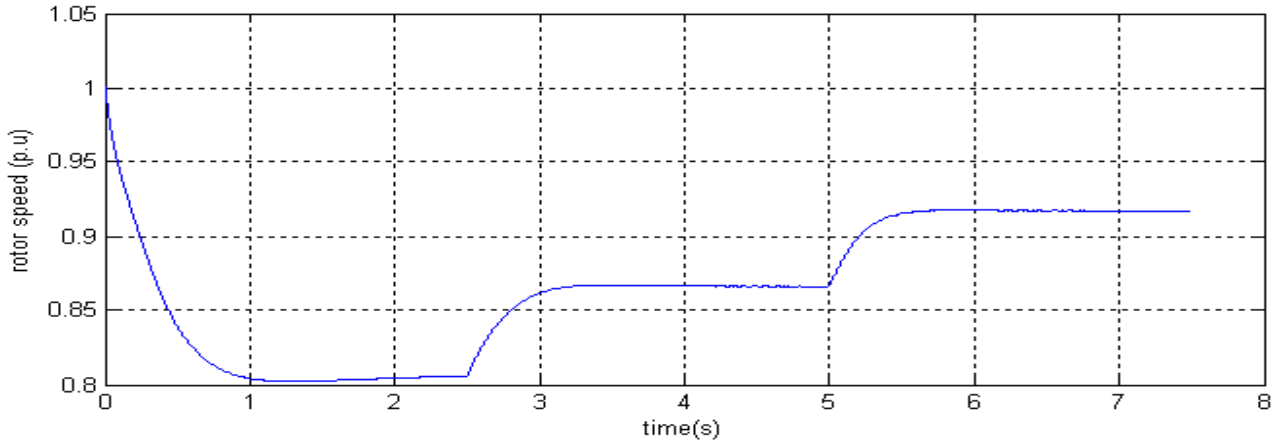

Figure (4.9) SEIG speed (p.u) using PI-controller

Figure (4.10) represents the change of Tip speed ration when using PI-controller. It is noted that there is little difference between the optimal value of Tip speed ratio and values where the control system using PI-controller. Where optimal value is equal 8.1 from the figure (4.10) when the wind speed is equal 8m/s the tip speed ratio is equal 8.1. Increasing wind speed leads to an increase in the Tip speed ration.

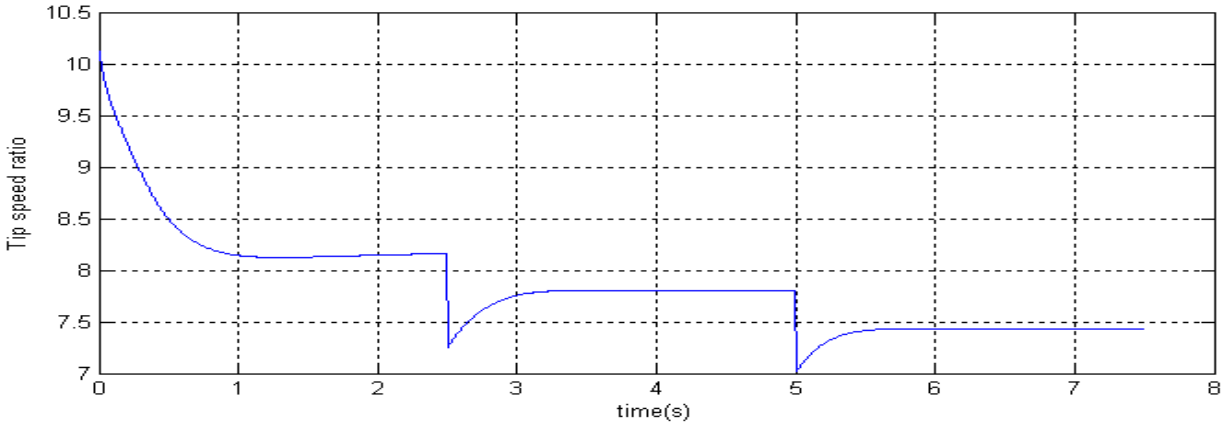

Figure (4.10) Tip speed ratio (λ) using PI-controller

Figure (4.11) represents the change in pitch angle of the wind turbine when using PI-controller. Note that the value of the pitch angle it is equal small value at first and then increased and then decline. Control system is change in the value of the pitch angle to make wind power generation system at maximum power available.

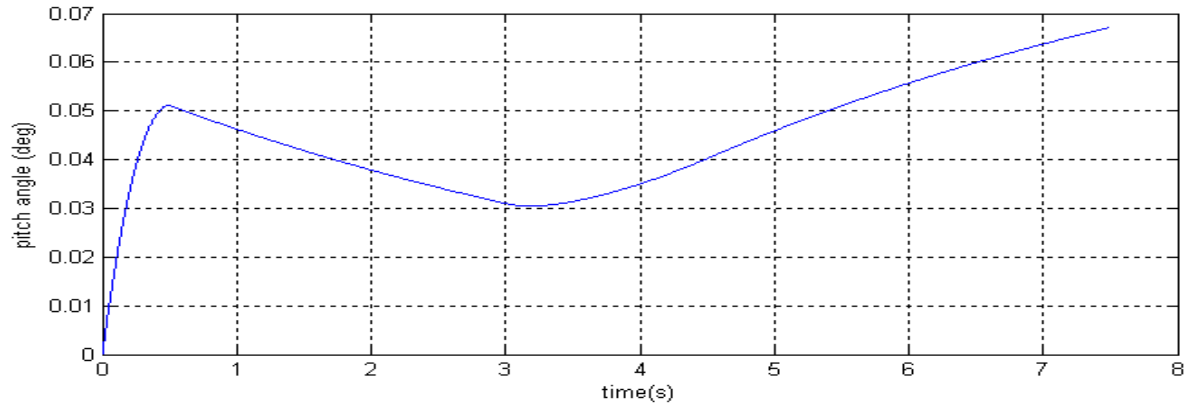

Figure (4.11) pitch angle with PI-controller

- **Comparison between PI-controller and PID-controller:**

The system is first operating at the wind velocity of 8m/s. The wind velocity is increased to 9 m/s, then the wind velocity is increased to 10 m/s where the values of various system variables at this speeds are shown in Tables (4.1), (4.2) and (4.3).

Table (4.1) Comparison between the PI-controller and PID-controller when the wind speed is 8m/sec

	With PI-controller	With PID-controller
Maximum power captured(W)	2818	2865
Power coefficient (C_P)	0.4787	0.48
Tip speed ratio (λ)	8.15	8.18
Rotor speed (p.u)	0.8058	0.8086
Pitch angle (deg)	0.05	0

Table (4.2) Comparison between the PI-controller and PID-controller, when the wind speed is 9m/sec

	With PI-controller	With PID-controller
Maximum power captured(W)	3906	3912
Power coefficient (C_P)	0.4765	0.4779
Tip speed ratio (λ)	7.796	7.799
Rotor speed (p.u)	0.8663	0.8666
Pitch angle (deg)	0.03	0

Table (4.3) Comparison between the PI-controller and PID-controller, when the wind speed is 10m/sec

	With PI-controller	With PID-controller
Maximum power captured(W)	5000	5000
Power coefficient (C_P)	0.4678	0.4696
Tip speed ratio (λ)	7.43	7.44
Rotor speed (p.u)	0.9172	0.9179
Pitch angle (deg)	0.04	0

From tables (4.1), (4.2) and (4.3), the system is first operating at wind velocity of V_{w1}=8m/s. At this velocity, the maximum power captured from the wind turbine is 2.818kW at t=2.3sec ,when using PI-controller, the maximum power captured is equal 2.856KW at t=2sec, when using the PID-controller, the wind velocity is increased to 9m/s, the maximum power corresponding to this velocity is 3.906kW. Again, at t=2.1sec

for the PI-controller and 3.912KW at t=1.7 sec for the PID-controller. When wind speed increased to 10m/s the maximum power captured is equal 5KW at 5.5sec in the both controller.

- As expected the PID- controller is faster than the PI-controller to get the optimal operating point,
- The pitch control based on PID- controller is able to extract more power from the PI-controller.
- The operating points get when using PID-controlled more stable then operating points which we get using PI- controller. PID-controller is better than PI-controller in the application of wind power generation to get the maximum power available in the wind speed.

4.3 Voltage and power characteristics of SEIG

The output voltage of SEIG depends up on the wind velocity and excitation capacitance values. Excitation capacitors are used to reduce the reactive power burden of self-excited squirrel cage induction generators.

Figure (4.12) shows the generated voltage of SEIG when applied the wind speed shown in figure (4.1) to the system. The generator produces 0.6p.u of the voltage when the wind speed is equal 8m/s ,0.8p.u of the voltage when the wind speed 9m/s and 1p.u of the voltage when the wind speed at rated value 10m/s. This output voltage is fed to the uncontrolled rectifier.

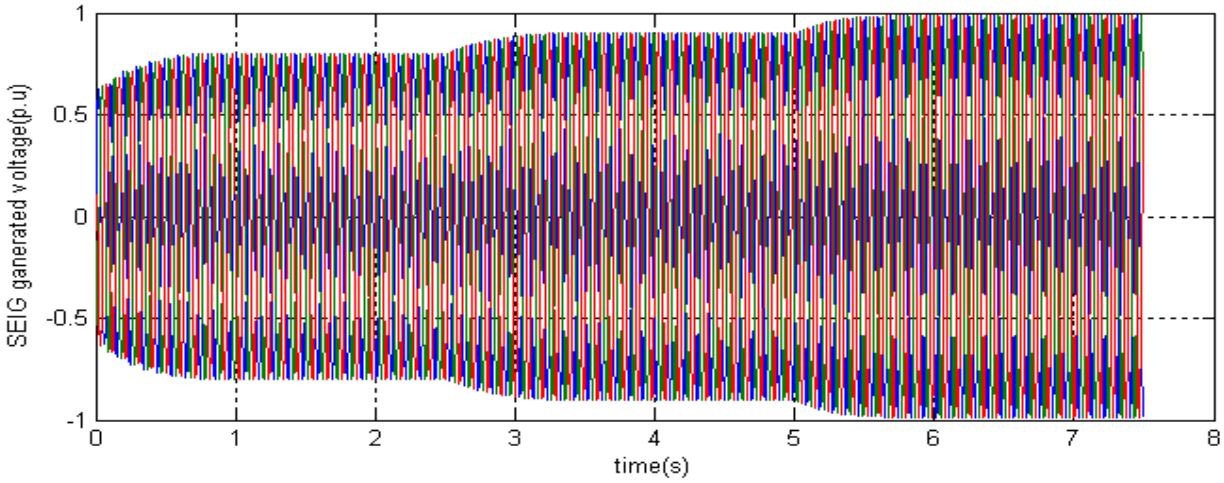

Figure (4.12) SEIG generated voltage

Figure (4.13) shows the output rectifier voltage applied to the inverter. The rectifier output voltage is 580V at wind speed 8m/s, 610V at wind speed 9m/s and 630V at wind speed 10m/s. A D.C link capacitor of 120μF in parallel with the diode maintains the voltage at an optimal value.

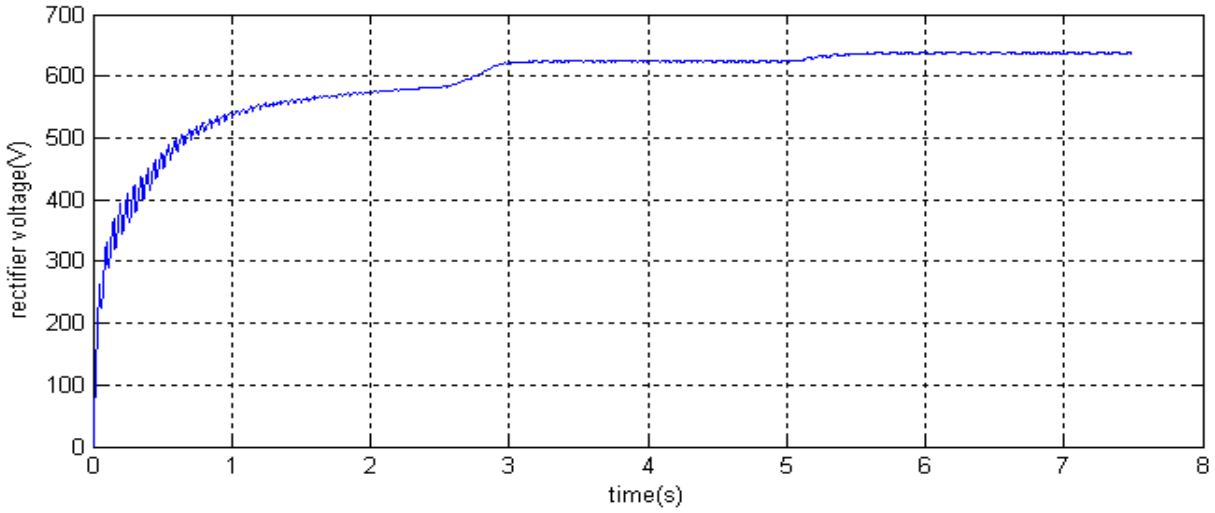

Figure (4.13): rectifier output voltage

Figure (4.14) shows the phase to phase output voltage waveform of the inverter. This inverter produces a required voltage with low harmonic distortion, the inverter produces (1p.u (380V r.m.s value)) in the output terminals. It took about 0.2sec to the settle to its steady state voltage. The controlled output voltage of the inverter is mainly depends upon the switching states. The output voltage of the inverter is controlled by pulse width modulation technique.

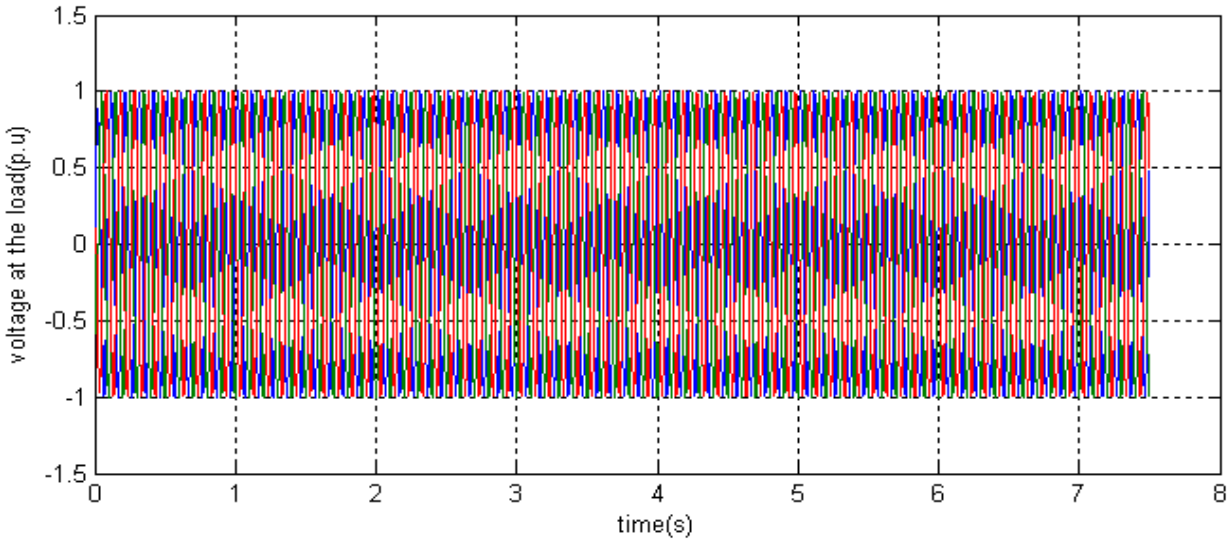

Figure (4.14) Voltage at the load

4.4 A case study of the loss of wind power

Wind power generation is several features but still the problem of wind power may not be available at all times and may be insufficient to generate electric power, so wind generation systems need to reserve units provide power for loads in case of loss of wind power and key reserve units used with wind power generation system of batteries of various types. This case study is to make sure that the battery system uninterrupted feeds electrical load when it loses wind generation system, open the main circuit breaker.

Battery storage system is essential for a stand-alone wind energy supply system to meet the required load power. As a variable speed wind energy system which has fluctuating generated power due to the variability of wind speed. It can store the excess energy when the generated power from the wind is more than the required load power for a time when the generated power from the wind is less than the required load power to maintain power balance between generated power and required load power. Also, it can remove the fluctuating power from wind energy system and maximize the reliability of power supplied to the load.

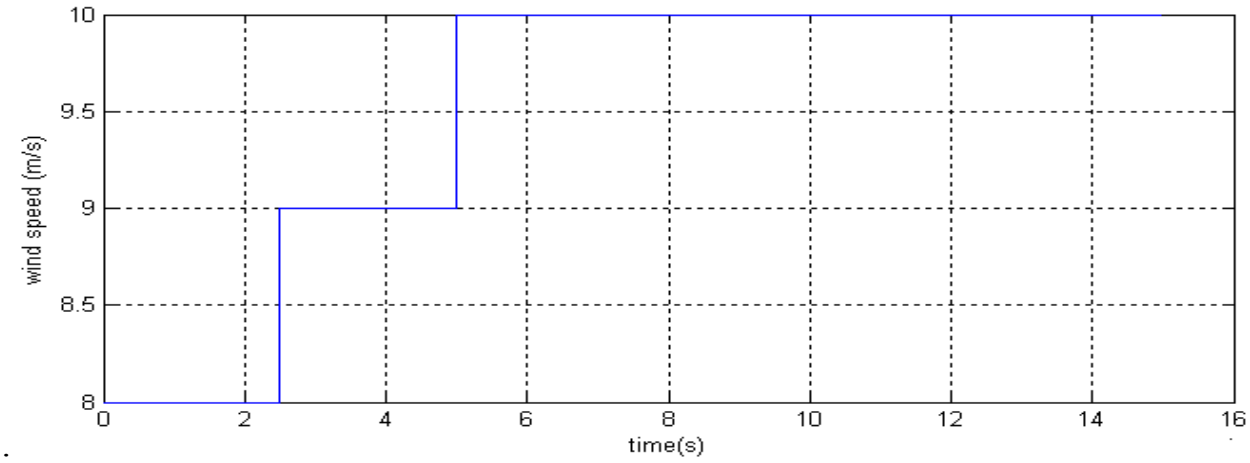

Figure (4.15) Variation of wind speed

Figure (4.15) represents the change in wind speed to be applied to the wind generation system to make sure that the backup battery system can be feed the electrical load when the loss of wind power.

Figure.(4.16) shows a voltage generated by the SEIG according to wind speed variations figure(4.15), at the wind speed of 8m/sec the generated voltage reaches to steady state value (0.6p.u) at 1sec , the wind velocity is increased to 9m/s the voltage corresponding

to this velocity (0.8p.u) at 3sec, at this wind velocity the main circuit backer is opened at 5sec,the voltage generated by SEIG is drop to zero after 1sec from open (C.B).

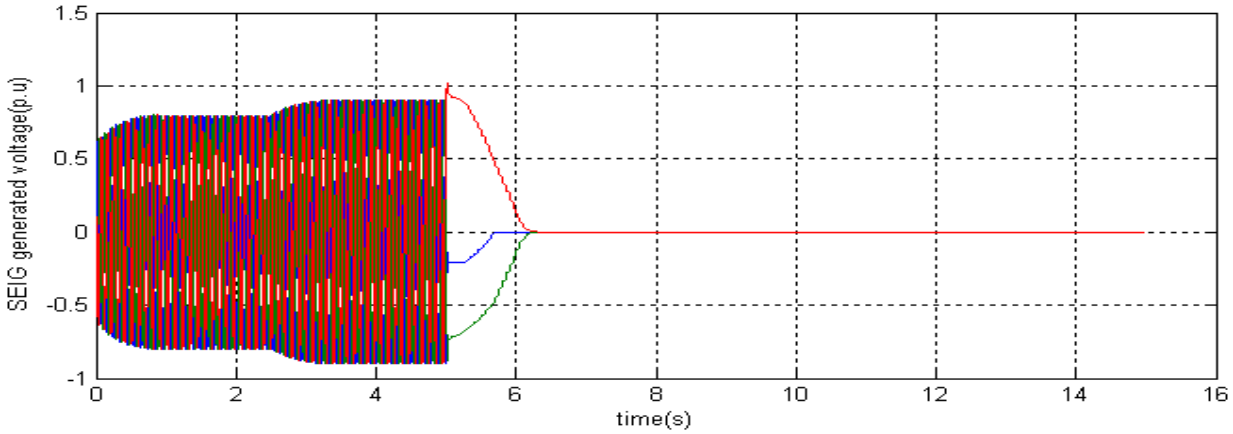

Figure (4.16) SEIG generated voltage when open main C.B

Figure (4.17) represent the voltage at load when open main C.B. It is noted that the voltage across the load was not affected by loss of generation by wind. This ensures uninterrupted system of batteries work on feeding electrical load.

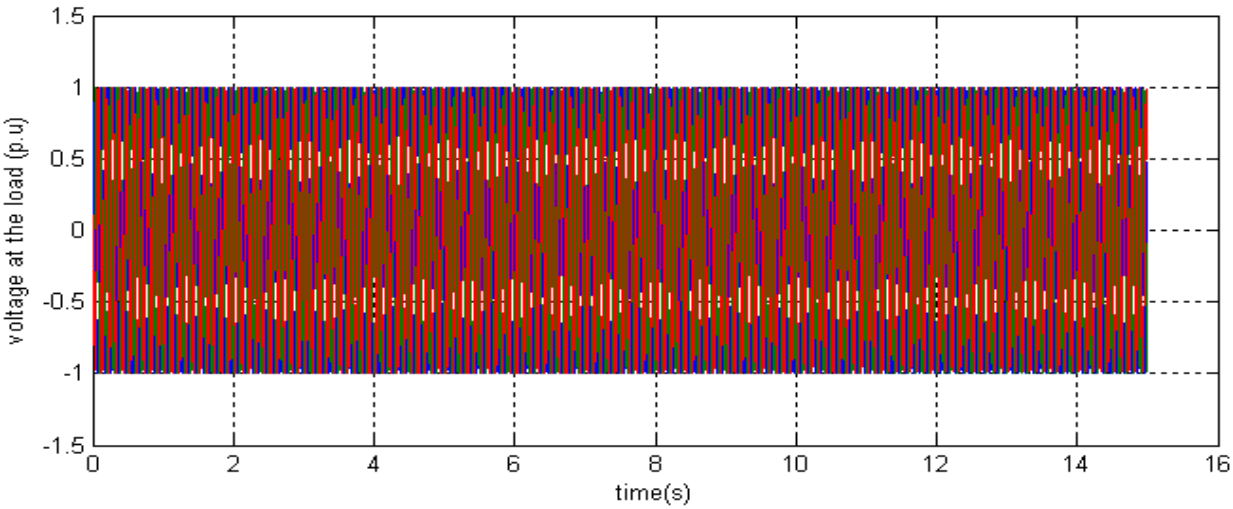

Figure (4.17): voltage at load when open main C.B

Figure (4.18) shows the output power of wind generation system. Note that the output power dropped to zero when the circuit barker is opened. Thus the loss of electrical power from wind generation system, if the system does not contain a backup feed system will stop electrical load.

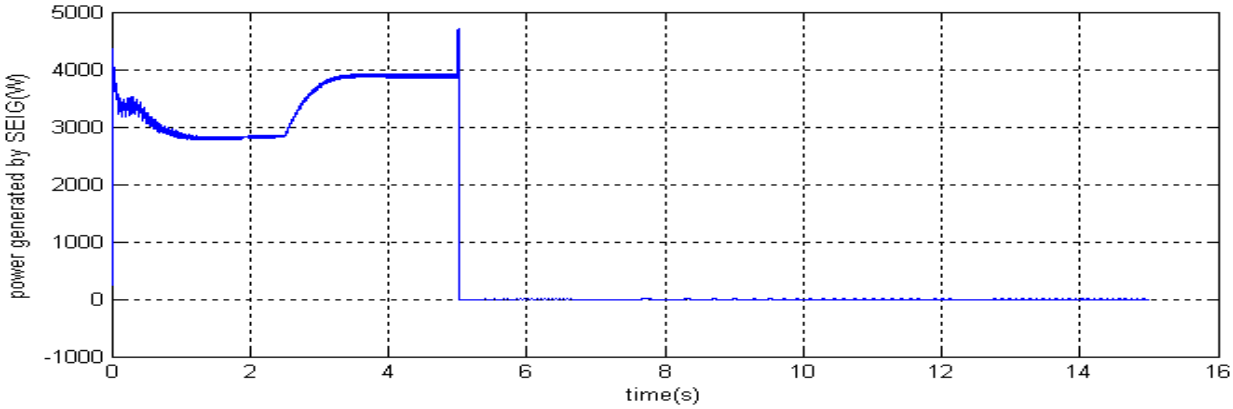

Figure (4.18): Active power generated by (SEIG) when opens main C.B

Figure (4.19) Shows the active power across the load when open (C.B). It is noted that the power of the electrical load was not affected by the loss of wind generation for the uninterrupted feeding system (batteries) to feed the electric load. Thus we make sure that uninterrupted feeding system has importance for wind generation systems

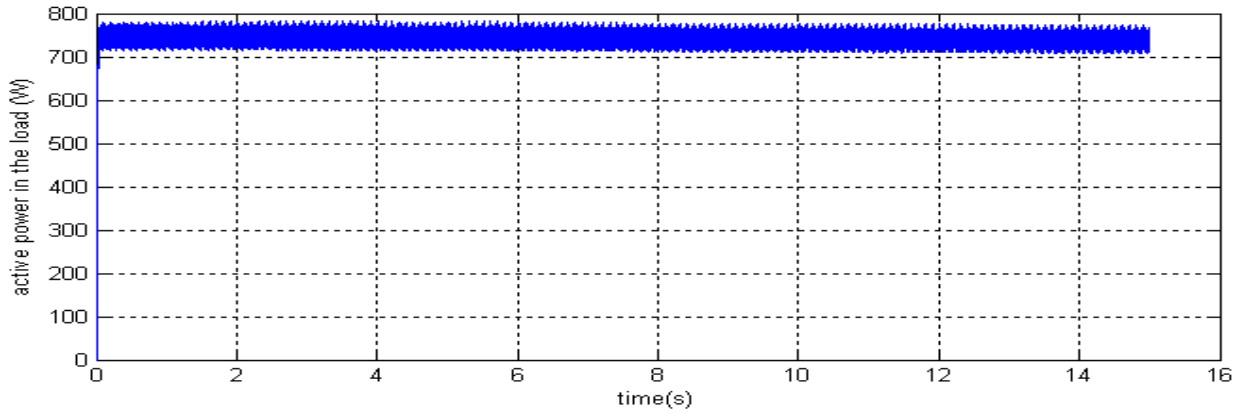

Figure (4.19): Active power in the load when open maim C.B

CHAPTER FIVE

CONCLUSIONS AND RECOMMENDATIONS

5.1 Conclusion

Control strategy of a stand-alone variable speed wind energy supply system has been presented in this thesis, along with a comprehensive analysis and simulation using MATLAB/SIMULINK. From the simulation results, the maximum power extraction control at the variable speed wind turbine has been implemented based on power signal feedback method (PSF), using the relation curve between generator speed and mechanical power to adjust the output power of wind turbine at optimum value through a pitch angle control for extracting maximum power from the available wind power. Also, the batteries banks have been able to store the surplus of wind energy and supply it to the load during a wind power shortage. Finally, it has been explained how the voltage source inverter controller uses a PWM strategy to supply controlled output voltage in terms of amplitude and frequency to the inductive load. The simulation results proved that the performance of the control strategy is satisfactory in spite of variation in wind speed.

5.2 Recommendations

- Use other methods to extracted maximum power tracking from available wind speed:
  - Hill Climb Search (HCS) method
  - Tip Speed Ratio (TSR) ratio method.
- Study and control of a variable –speed wind turbine energy system connected to the grid.
- Use other methods of controller for example fizzy logic control or robust control.

References

[١] Sunil Kumar,Shivani Sehgal,Sagar Bhosle, "Voltage and Frequency Control of SEIG in Small Wind Power Plant Using VFC" ,International Journal of Advanced Research in Electrical, Electronics and Instrumentation Engineering, Vol. 2, Issue 8, August 2013.

[٢] Mahmud M. Hussein,TomonobuSenjyu, Mohamed Orabi "Control of a Stand-Alone Variable Speed Wind Energy Supply System " ,applied sciences ISSN 2076-3417 , Appl. Sci. 2013, 3, 437 456; doi:10.3390/app3020437

[٣] Mohamed Mansour, M. N. Mansouri , M.F. Mmimouni,"Study and Control of a Variable-Speed Wind-Energy System Connected to the Grid" ,International Journal Of Renewable Energy Research, IJRER., Vol.1, No.2, pp.96-104 ,2011.

[٤] Mukund R. Patel "Wind and solar power system",Boca Raton London New York Washington, D.C, 1999.

[٥] José Antonio Barrado, Robert Griñó, "Analysis of voltage control for a self-excited induction generator using a three-phase four-wire electronic converter" ,University at Rovira Virgili, (España) .

[٦] Karim H. Youssef, Manal A. Wahba, Hasan A. Yousef and Omar. A. Sebakhy, "A New Method for Voltage and Frequency Control of Stand-Alone Self-Excited Induction Generator Using PWM Converter with Variable DC link Voltage" ,American Control Conference Westin Seattle Hotel, Seattle, Washington, USA June 11-13, 2008.

[٧] International Energy Agency (IEA) ,"Technology Roadmap wind energy" 2013 edition.

[٨] Kathryn E. Johnson "Adaptive Torque Control of Variable Speed Wind Turbines", National Renewable Energy Laboratory 1617 Cole Boulevard, Aug. 2004

[٩] B H Khan "Non-conventional energy resources" ,by Tata McGraw-Hill companies, first edition, 2006.

[١٠] Kathryn E. Johns "Methods for Increasing Region 2 Power Capture on variable-Speed Wind Turbine", Journal of Solar Energy Engineering, 20 Feb 2008 to 128.138.64.178

[١١] AbdulhamedHwas and Reza Katebi "Wind Turbine Control Using PI Pitch Angle Controller", IFAC Conference on Advances in PID Control, Brescia (Italy), March 28-30, 2012

[١٢] Marcelo Gustavo Molina and Pedro Enrique Mercado "Modeling and Control Design of Pitch-Controlled Variable Speed Wind Turbines ",Universidad National de San Juan Argentina, April, 2011.

[1٣] Alireza Nami and firuzzare, "Multilevel converters in renewable energy systems ", Queensland University in Australia, ISBN: 978-953-619-52-7, 2009.

[١٤] Swati Devabhaktuni, S.V.JayaramKuma "Modeling and Analysis of Wind turbine Driven Self-Excited Induction Generator Connected to Grid Interface with Multilevel H-Bridge Inverter" ,Journal of Energy Technologies and Policy ISSN 2224-3232 (Paper) ISSN 2225-0573 Vol.2, No.2, 2012.

[١٥] S. Masoud Barakati "Modeling and Controller Design of a Wind Energy Conversion System Including A Matrix Converter", A thesis presented to the University of Waterloo Ontario, Canada, 2008.

[١٦] K.Subramanian, S.P. Sabberwal "Cost Effective Wind Energy Conversion Scheme Using Self Excited Induction Generator", Trans Tech Publications , Advanced Materials Research Vol. 768 (2013) pp 143-150(2013).

[17] Tony burton,Nick Jenkins, davidsharpe ,Ervin bossanyi "wind energy handbook" ,library of congers cataloguing , second edition,2011.

[18] Gary L.johnson "wind energy system", library of congers cataloguing, America electronic edition, December 2001.

[19] Thomas Ackermam "wind power in power system ", johnwiley and sons, let, England , first edition, 2005.

[20] Mohammad Shahrokhi and Alireza Zomorrodi "Comparison of PID Controller Tuning Methods" ,Sharif University of Technology, December 2007

Appendix:

Appendix shows the data of model.

Generator data	

Nominal power	4.7KW		
Line to line volt	460V rms value		
Frequency	60 HZ		
Stator resistance	0.01965p.u		
Stator inductance	0.0397p.u		
Rotor resistance	0.01909p.u		
Inductance resistance	0.0397pu		
Magnetizing Inductance	1.354p.u		
Inertia	0.09526s		
Friction factor	0.05479p.u		
Pairs' of poles	2		
Excitation reactive power	2KVAR		
Turbine data:			
Nominal mechanical output power	4.7KW		
Base wind speed	1p.u		
Maximum power at based wind	1p.u		
Reference pitch angle	0 angle		
Control parameter:			
Gain of PID-controller	K_p	K_i	K_d
Speed regulator	0.001	0.01	0.001
Pitch angle regulator	1	1	5
Current regulator	0.01	0.03	0.1

Control parameter:			
Gain of PI-controller	K_p	K_i	
Speed regulator	5	1	

Pitch angle regulator	1	1	
Current regulator	1	5	